Polar Geosci., **12**, 101–125, 1999

GEOCHEMICAL STUDY OF GRANULITES FROM MT. RIISER-LARSEN, ENDERBY LAND, EAST ANTARCTICA: IMPLICATION FOR PROTOLITHS OF THE ARCHAEAN NAPIER COMPLEX

Satoko SUZUKI[1], Tomokazu HOKADA[1], Masahiro ISHIKAWA[2] and Hideo ISHIZUKA[3]

[1]*Department of Polar Science, School of Mathematical and Physical Sciences, The Graduate University for Advanced Studies, Kaga 1-chome, Itabashi-ku, Tokyo 173-8515*
[2]*Geological Institute, Yokohama National University, Tokiwadai, Hodogaya-ku, Yokohama 240-8501*
[3]*Department of Geology, Kochi University, Akebono-cho 2-chome, Kochi 780-8520*

Abstract: The Mt. Riiser-Larsen area of the Napier Complex, East Antarctica, is underlain by various kinds of ultrahigh-temperature (UHT) metamorphic rocks such as orthopyroxene felsic gneiss, garnet felsic gneiss, garnet-sillimanite gneiss, mafic gneiss and meta-ultramafic rocks. On the basis of the mode of occurrence and petrography, the garnet felsic gneisses are further divided into garnet felsic gneiss I (garnet-poor type) and II (garnet-rich type), the mafic gneisses into quartz-free and -bearing types, and the meta-ultramafic rocks into phlogopite-free and -bearing types. Bulk rock chemical analyses for the major, minor and rare earth elements (REEs) demonstrate that (1) both the garnet-sillimanite gneiss and garnet felsic gneiss II are of sedimentary origin such as mudstone and sandstone, respectively, and (2) other rocks are of igneous origin, as follows: i) the orthopyroxene felsic gneiss and garnet felsic gneiss I are chemically comparable with CIPW normative tonalite to granodiorite and granite, respectively, of which the former also exhibits a calc-alkaline compositional variation with a REE signature comparable to the Archaean TTG (tonalite-trondhjemite-granodiorite); ii) the quartz-free and quartz-bearing mafic gneisses have been derived from flat or slightly LREE-depleted and LREE-enriched tholeiitic basalts, respectively; iii) phlogopite-free and phlogopite-bearing meta-ultramafic rocks have been derived from depleted mantle peridotites and komatiitic rocks, respectively, of which the latter shows a magmatic compositional variation controlled by addition or subtraction of only olivine. These chemical features reveal that the various kinds of original rocks are intermingled in the Riiser-Larsen area, which is important for understanding the site of development of original rocks in the Napier Complex.

key words: bulk rock chemistries, Mt. Riiser-Larsen, Napier Complex, original rocks, ultrahigh-temperature metamorphic rocks

1. Introduction

The Napier Complex in Enderby Land, East Antarctica (Fig. 1), consists mainly of the upper granulite facies rocks metamorphosed during the late Archaean to early Proterozoic age (SHERATON *et al.*, 1987), and contains such unique minerals and mineral assemblages as osumilite, inverted pigeonite, sapphirine+quartz, and garnet+sillimanite+

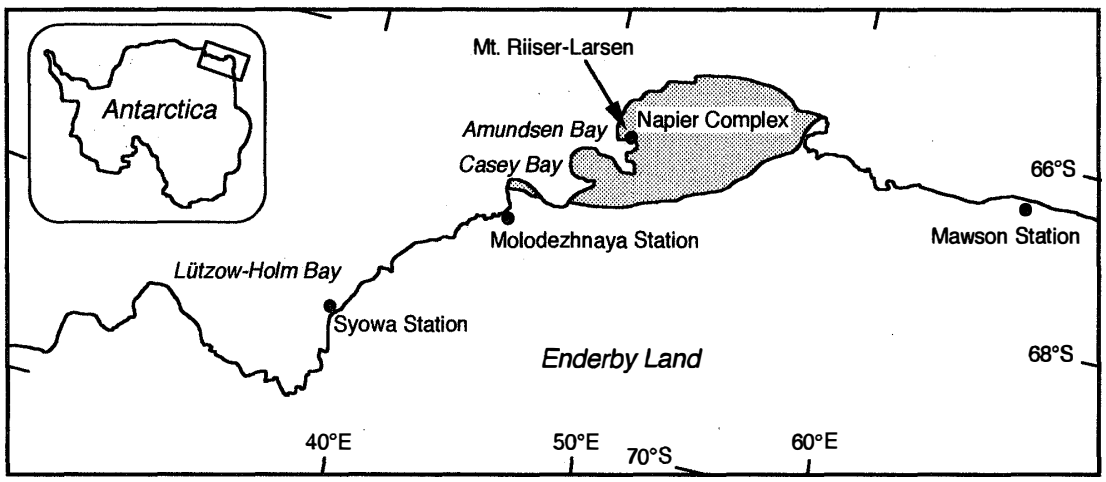

Fig. 1. Index map of the Riiser-Larsen area, Enderby land, East Antarctica.

orthopyroxene (*e.g.*, DALLWITZ, 1968; ELLIS, 1980; GREW, 1980, 1982; SANDIFORD and POWELL, 1986; HARLEY, 1987; HARLEY and HENSEN, 1990). This implies that the Napier Complex represents an extremely high temperature (ultrahigh-temperature as high as 1000°C or even more) metamorphic terrane. Furthermore, the ion microprobe U-Pb dating of zircon from orthogneiss yields an age as old as 3800 Ma for the granodioritic to tonalitic precursor (BLACK *et al.*, 1986; HARLEY and BLACK, 1997). The Napier Complex is thus particularly important in understanding the nature of ultrahigh-temperature (UHT) metamorphism as well as its role in Archaean crustal growth and differentiation.

The Mt. Riiser-Larsen area (66°47′S, 50°42′E) is located on the eastern coastline of Amundsen Bay (Figs. 1 and 2). On the basis of the unique minerals and mineral assemblages described above (MOTOYOSHI and MATSUEDA, 1984, 1987; MAKIMOTO *et al.*, 1989; MOTOYOSHI and HENSEN, 1989; MOTOYOSHI *et al.*, 1990), this area has been inferred to represent the highest metamorphic grade portion within the Napier Complex (HARLEY and HENSEN, 1990). Recently, the area has been geologically mapped in detail for the first time (ISHIZUKA *et al.*, 1998). Following up this geological study, the present study is aimed to explore major, minor and rare earth elements of the ultrahigh-temperature metamorphic rocks in the Mt. Riiser-Larsen area in order to characterize the nature of their protoliths in terms of the geochemical constraints.

2. Geological Outline and Sample Descriptions

The simplified geologic map of the Mt. Riiser-Larsen area modified after ISHIZUKA *et al.* (1998) is shown in Fig. 2. The area is mainly composed of the layered gneiss series (LGS) in the central to northwestern part while its southern to southeastern part is mainly occupied by the massive gneiss series (MGS). However, these two gneiss series are not mutually exclusive, and indeed, transitional varieties occur between the two gneiss series, which are referred to collectively as the transitional gneiss series (TGS). The columnar sections showing the details of field occurrences of LGS are illustrated in Figs. 3A and 3B, of which Fig. 3B includes the section shown in Fig. 4A. The following is brief descriptions of field occurrence and petrography of the samples analyzed here;

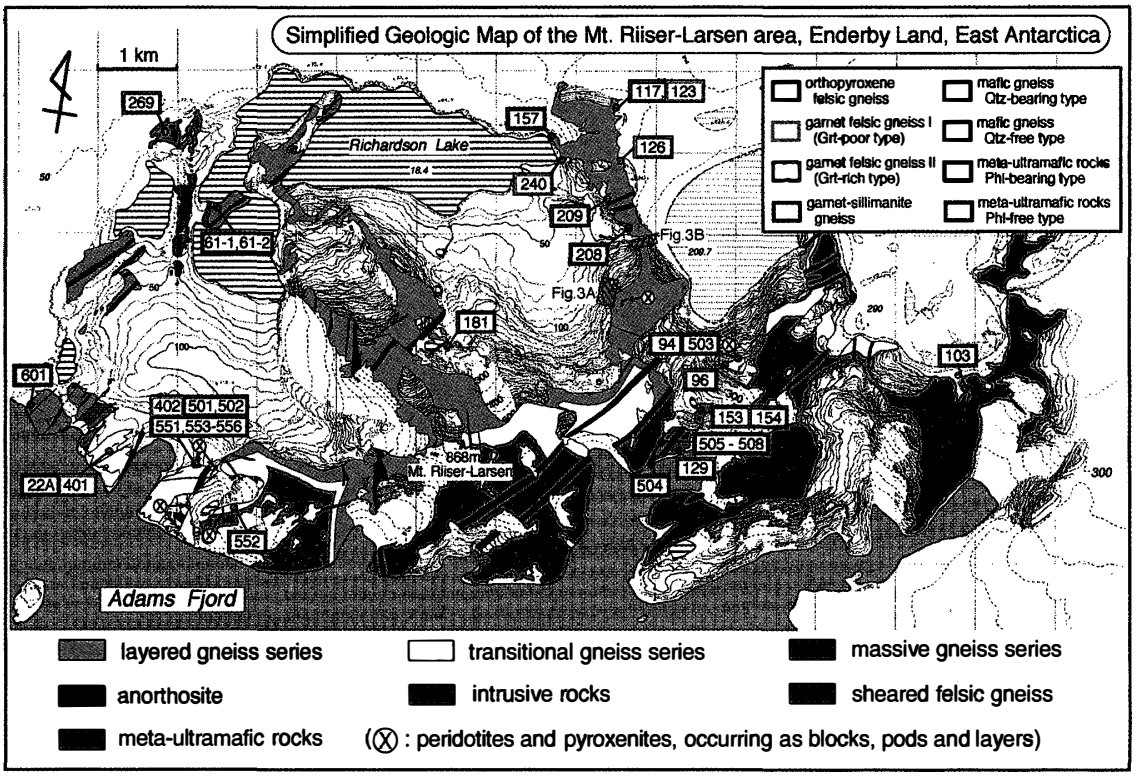

Fig. 2. Simplified geologic map of the studied area (modified after ISHIZUKA *et al., 1998) along with localities of samples analyzed in this study. Numerals in squares are sample numbers.*

the generalized descriptions of geology and petrography have been given by ISHIZUKA *et al.* (1998). The range of modal proportions of representative minerals is shown in the parenthesis.

Orthopyroxene felsic gneiss: The orthopyroxene felsic gneiss is predominant in the MGS, but also occurs as layers with various thicknesses in the LGS. It is generally massive, but sometimes displays weak lineation defined by elongated quartz. Irregular-shaped patches of mafic gneisses are rarely included in the orthopyroxene felsic gneiss (Fig. 4B). On the basis of feldspar composition, SHERATON *et al.* (1987) classified the orthopyroxene felsic gneisses of the Napier Complex into a potassic variety containing mesoperthite and a calcic variety that is predominant in plagioclase. The orthopyroxene felsic gneisses analyzed here consist of orthopyroxene (2–8%), mesoperthite (60–70%), plagioclase (1–3%), quartz (20–30%), and minor zircon, monazite, apatite, ilmenite and magnetite (Fig. 5A), which are equivalent to the potassic variety of SHERATON *et al.* (1987).

Garnet felsic gneiss: The garnet felsic gneiss is a predominant lithology in the LGS, forming layers with various thicknesses. The modal proportion of constituent minerals, especially garnet, is highly variable, which gives rise to variation of rock color in the field. Here we subdivide the garnet felsic gneiss into garnet felsic gneiss I (garnet-poor type) and II (garnet-rich type). The garnet felsic gneiss I is mainly composed of garnet (2–10%), quartz (25–40%) and perthite to mesoperthite (50–65%), and is grayish pink in color (Fig. 4C). The garnet felsic gneiss II mainly consists of garnet (12–20%),

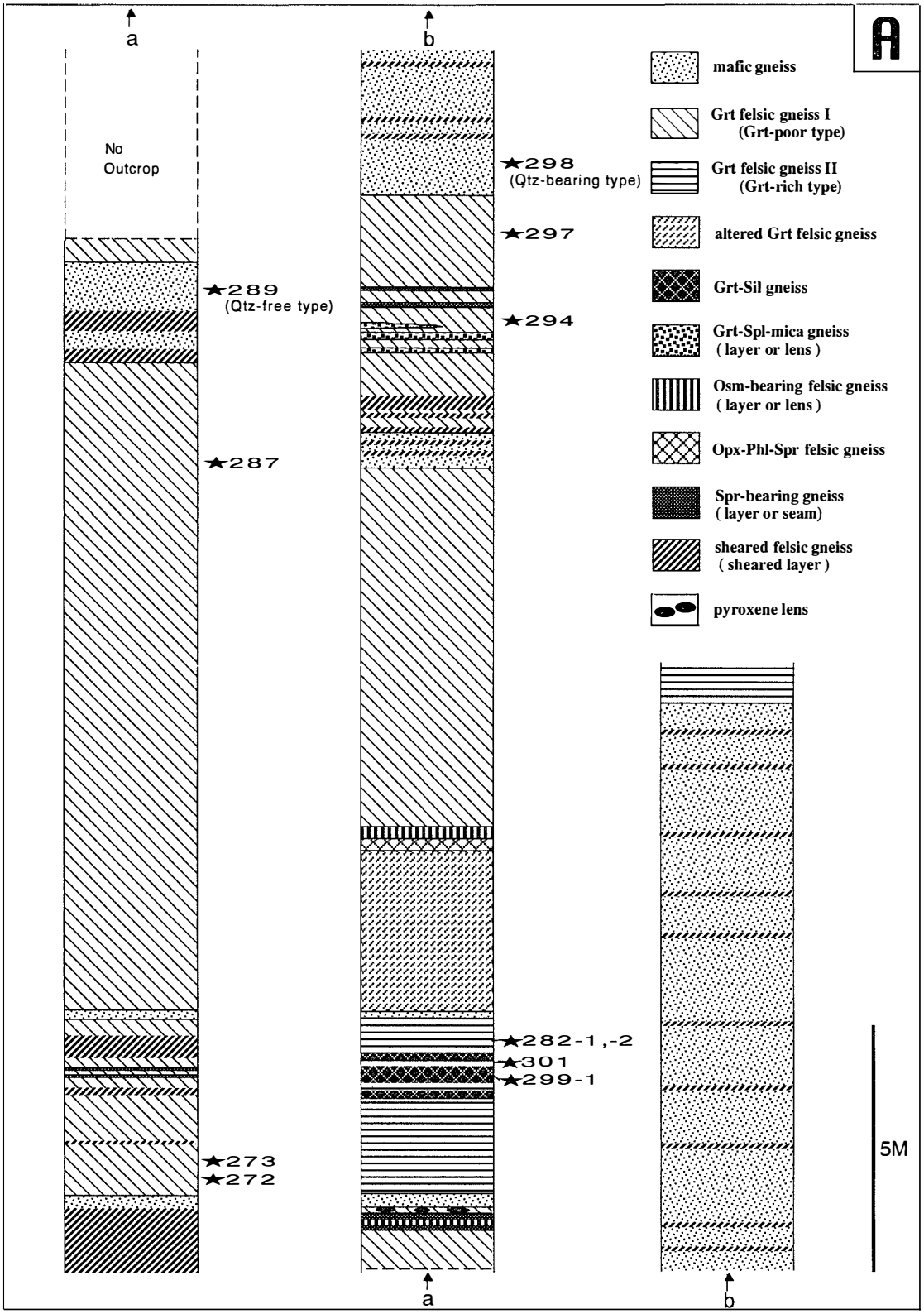

Fig. 3. Lithostratigraphic columns of the layered gneiss series with the localities of samples analyzed in this study. A and B correspond to the areas shown in Fig. 2, respectively. Numbers with stars represent sample numbers (No.).

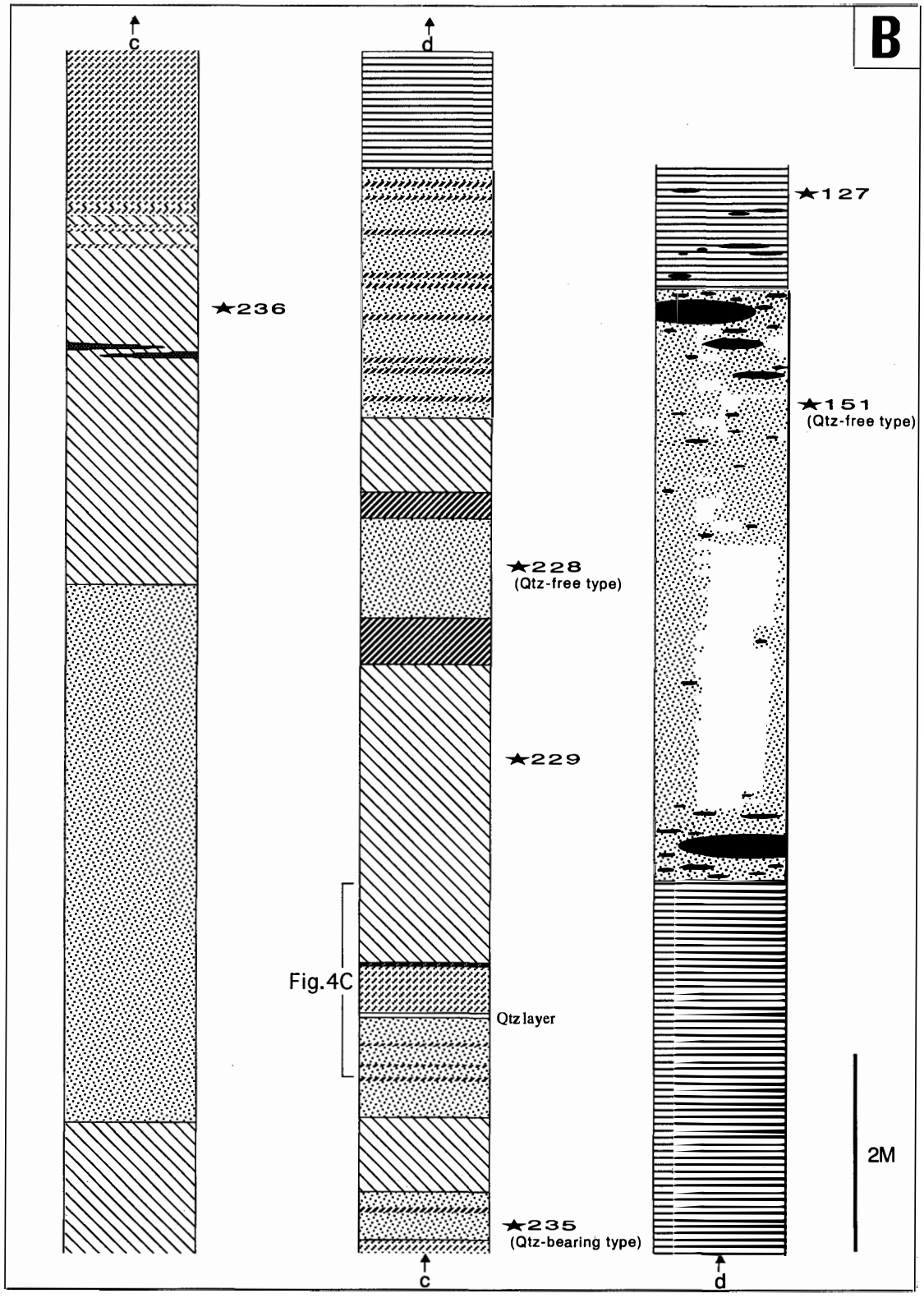

Fig. 3 (continued).

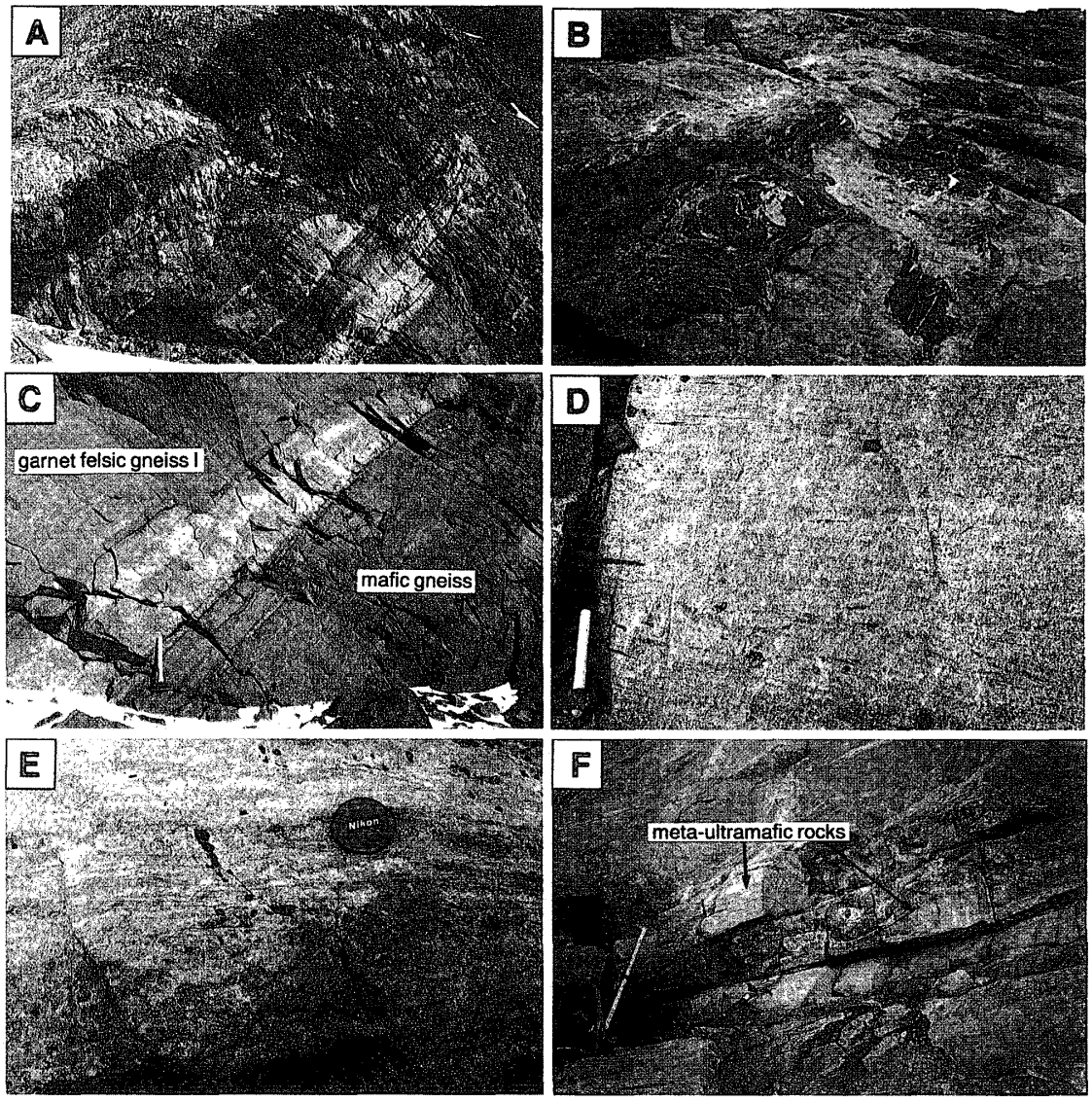

Fig. 4. Field occurrences of representative metamorphic rocks in the Mt. Riiser-Larsen area. A: Well developed layering structure consisting mainly of mafic gneiss, garnet felsic gneiss, and minor sapphirine-bearing pools. The area of the photograph is included in Fig. 3B, and the width of the field of view is approximately 40 m. B: Orthopyroxene felsic gneiss with irregular-shaped patches of mafic gneiss. C: Garnet felsic gneiss I interlayered with mafic gneiss. D: Garnet felsic gneiss II. E: Garnet-sillimanite gneiss. F: Meta-ultramafic rock forming thin layers within the orthopyroxene felsic gneiss.

quartz (28–45%) and perthite to mesoperthite (40–52%), and is orange in color (Fig. 4D). These minerals are medium- to coarse-grained with granoblastic texture. Accessory minerals include xenotime, apatite, zircon, monazite, rutile and ilmenite in the garnet felsic gneiss I (Fig. 5B), and spinel, zircon, rutile and ilmenite in the garnet felsic gneiss II (Fig. 5C).

Garnet-sillimanite gneiss: The garnet-sillimanite gneiss rarely occurs in the LGS, forming thin layers with thickness ranging from a few centimeters to several tens of centimeters, or small pools within the garnet felsic gneiss (Fig. 4E). Particularly, the

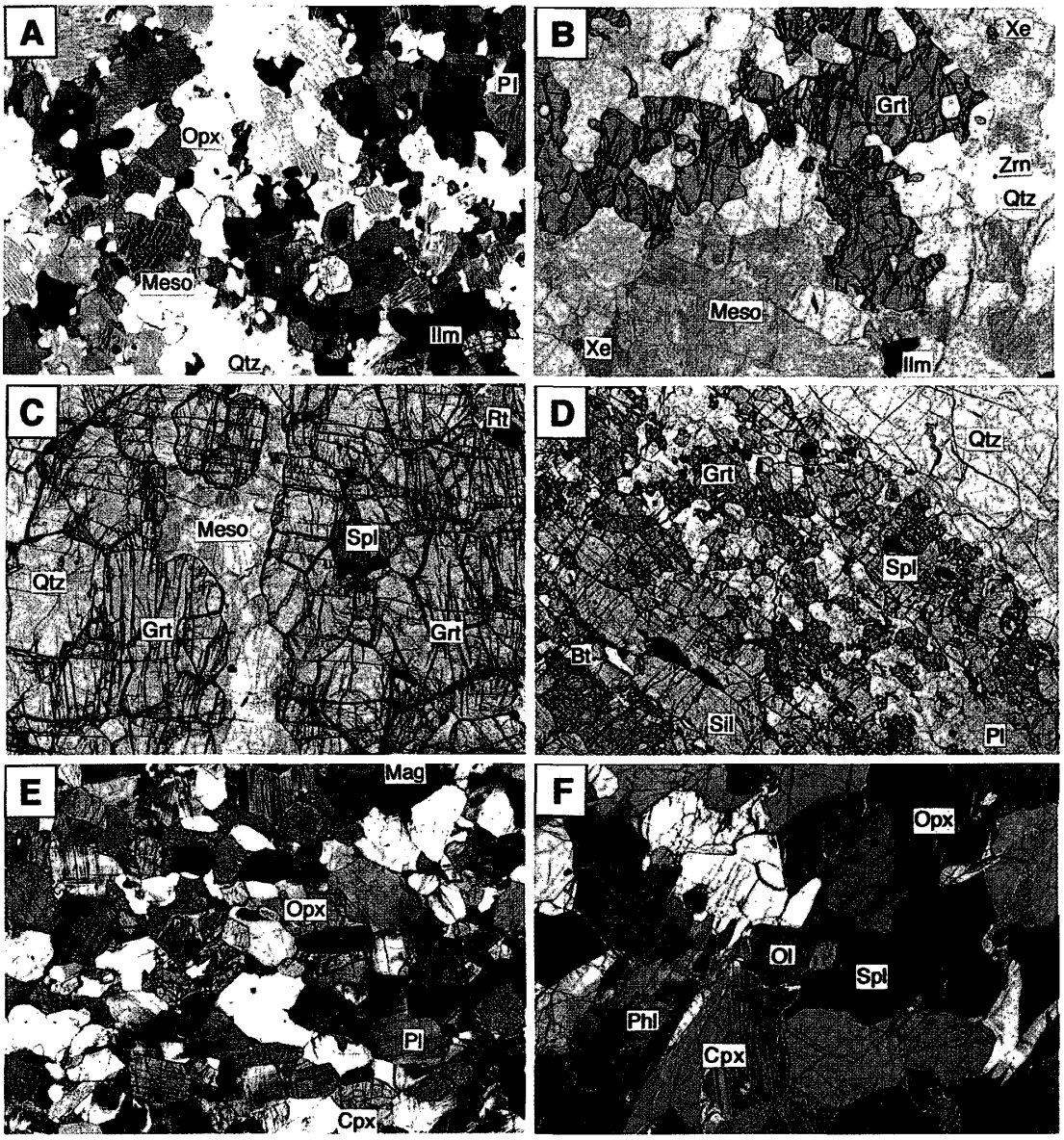

Fig. 5. Photomicrographs of representative metamorphic rocks in the Mt. Riiser-Larsen area. A: Orthopyroxene felsic gneiss (width=6 mm). B: Garnet felsic gneiss I (width=6 mm). C: Garnet felsic gneiss II (width=6 mm). D: Garnet-sillimanite gneiss (width=1.2 mm). E: Mafic gneiss (width=1 cm). F: Meta-ultramafic rock (width=4 mm). Abbreviations: Bt=biotite, Cpx=clinopyroxene, Grt=garnet, Ilm=ilmenite, Mag=magnetite, Meso= mesoperthite, Ol=olivine, Opx=orthopyroxene, Phl=phlogopite, Pl=plagioclase, Qtz=quartz, Rt=rutile, Spl=spinel, Xe=xenotime, Zrn=zircon.

garnet-sillimanite gneiss occurs closely associated with the garnet felsic gneiss II, sometimes in small-scale alternation. The constituent minerals include garnet, sillimanite, spinel, sapphirine, osumilite, cordierite and biotite with subordinate amounts of feldspar, quartz, zircon and magnetite (Fig. 5D); the modal proportion of the main constituents is highly variable. Of these, garnet is usually coarse-grained, being up to 10 cm in diameter, and prismatic sillimanite commonly displays preferred orientation.

Mafic gneiss: The mafic gneiss occurs mainly in the LGS, and is commonly inter-

layered with the garnet felsic gneiss and sometimes orthopyroxene felsic gneiss, having a thickness of a few centimeters to a few meters (Fig. 4C). Occasionally, it forms layers slightly oblique to the neighboring garnet felsic gneiss, suggesting an intrusive origin for its precursor. Most of the mafic gneisses are medium in grain size and granoblastic in texture (Fig. 5E). On the basis of accessory quartz, the mafic gneisses are further divided into quartz-free and quartz-bearing types. The quartz-free and -bearing types are mainly composed of plagioclase (55–68% and 55–65%), clinopyroxene (16–30% and 28–32%) and orthopyroxene (7–12% and <7%). Accessory minerals include apatite, ilmenite, and magnetite. The quartz-free type is dark-gray while the quartz-bearing type is light-gray in color, which is, however, ambiguous at times.

Meta-ultramafic rocks: The meta-ultramafic rocks occur sporadically mainly in the TGS as lenticular or rounded blocks, rarely forming thin layers within the orthopyroxene felsic gneiss (Fig. 4F). The main constituent minerals include olivine, orthopyroxene and clinopyroxene (Fig. 5F). Some meta-ultramafic rocks also contain small amounts of phlogopite (0.1–1.0%); the meta-ultramafic rocks occurring as thin layers are commonly phlogopite-bearing. On the basis of the modal proportions of olivine, orthopyroxene and clinopyroxene (Fig. 6), the phlogopite-free type is classified into dunite, harzburgite and olivine orthopyroxenite, and the phlogopite-bearing type into dunite, lherzolite, olivine websterite and websterite. These constituent minerals are medium- to coarse-grained and equigranular. Accessory minerals include spinel and magnetite.

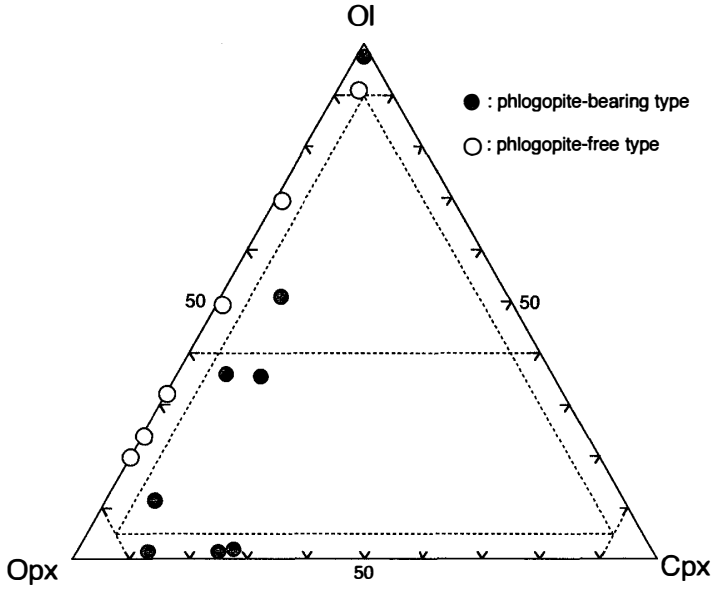

Fig. 6. Modal proportion of meta-ultramafic rocks.

3. Bulk Rock Chemistries

The bulk rock analyses for the major and minor elements were performed by using an X-ray fluorescence analyzer (XRF) (Rigaku RIX-3000) at the National Institute of Polar Research. The analytical procedure followed the methods of MOTOYOSHI and SHIRAISHI (1995) and MOTOYOSHI *et al.* (1996). The rare earth elements (REEs) of bulk

Table 1. Bulk rock analyses of the metamorphic rocks from the Mt. Riiser-Larsen area.

Sample No.	103	96	129	153	94	209	294	273	236	287	272	229	402
Rock Facies	*orthopyroxene felsic gneiss*						*garnet-poor garnet felsic gneiss*						
Mineral Assemblage	Opx, Meso Pl, Qtz, Ap Zm, Ilm	Opx, Meso Pl, Ap, Zm, Ilm	Opx, Meso Pl, Qtz, Ap Zm, Ilm, Mag	Opx, Meso Pl, Qtz, Ap Zm, Ilm, Mag	Opx, Meso Pl, Qtz, Ap Zm, Ilm	Opx, Meso Pl, Qtz Zm, Ilm	Grt, Meso, Pl Xe, Zm, Mo Qtz, Ilm, Rt	Grt, Meso Xe, Zm, Mo Qtz, Ilm	Grt, Meso Xe, Zm, Mo Qtz, Ilm	Grt, Meso, Pl Xe, Zm, Mo Qtz, Ilm, Rt	Grt, Meso, Pl Xe, Zm, Mo Qtz, Ilm, Rt	Grt, Meso, Pl Xe, Zm, Mo Qtz, Ilm, Rt	Grt, Meso, Pl Xe, Zm, Mo Qtz, Ilm
(wt.%)													
SiO2	64.16	67.76	69.19	70.59	70.97	71.38	68.15	72.11	72.81	73.76	73.93	74.49	75.41
TiO2	0.76	0.32	0.45	0.33	0.30	0.33	0.33	0.12	0.33	0.30	0.13	0.29	0.18
Al2O3	17.37	13.23	15.48	15.46	15.19	15.12	16.26	13.79	13.84	13.86	13.97	12.75	13.22
Fe2O3	4.46	6.11	3.92	2.44	2.64	2.33	4.12	3.28	3.46	2.59	2.74	3.03	2.33
MnO	0.04	0.10	0.05	0.04	0.03	0.01	0.02	0.02	0.02	0.02	0.02	0.03	0.02
MgO	1.34	3.26	1.23	0.99	1.37	0.94	1.04	0.56	0.54	0.45	0.56	0.38	0.32
CaO	5.31	3.21	4.12	3.18	3.96	3.03	1.86	1.20	1.58	1.25	1.09	1.38	1.67
Na2O	4.43	3.59	4.22	4.09	4.17	3.82	3.08	2.64	2.55	2.71	2.70	2.53	2.79
K2O	1.49	1.61	1.23	2.66	1.21	2.73	5.00	5.02	4.59	5.19	5.37	4.33	3.87
P2O5	0.29	0.09	0.12	0.07	0.05	-	0.07	0.04	0.04	0.08	0.04	0.09	0.03
Total	99.65	99.27	100.02	99.83	99.89	99.69	99.93	98.78	99.76	100.20	100.55	99.29	99.84
(ppm)													
Ba	536.7	1252	260.7	1516	977.8	2103	741.2	786.4	588.3	865.9	801.4	910.0	623.0
Co	14.8	23.2	11.5	9.4	11.2	6.8	11.0	7.1	7.9	5.3	5.0	5.5	4.1
Cr	3.5	246.2	5.2	14.9	27.2	35.6	15.1	8.1	18.2	2.1	1.9	12.0	10.4
Cu	23.9	4.6	1.0	7.9	6.1	9.5	0.5	6.5	2.0	2.7	2.1	3.1	4.1
Nb	12.1	6.2	12.1	4.2	3.4	3.9	17.0	10.4	29.1	35.6	7.6	27.3	3.9
Ni	88.2	70.4	18.8	41.4	55.9	28.1	4.6	6.0	4.7	4.2	3.6	9.2	4.0
Rb	15.6	12.9	14.9	39.8	5.7	29.6	167.5	164.1	141.2	180.6	181.7	171.7	90.5
Sr	273.6	259.8	169.0	294.2	324.9	353.8	91.2	64.1	60.9	79.6	63.4	62.4	94.8
V	46.2	46.6	40.7	24.1	24.9	31.0	11.4	4.2	13.1	9.3	6.0	6.5	13.2
Y	14.9	11.4	17.3	3.0	3.0	0.2	127.3	155.7	154.1	123.2	127.6	155.9	92.3
Zn	55.6	99.5	64.0	33.1	33.5	29.7	25.9	24.5	22.8	20.9	19.8	30.6	16.7
Zr	312.2	119.7	231.8	138.1	154.1	18.6	325.2	225.1	268.8	284.0	285.6	236.8	223.1
Ga	20	17	19	15	14	17	31	20	22	17	19	23	18
Ge	0.7	1.1	0.8	0.8	0.7	0.5	1.4	1.6	1.5	1.1	1.2	1.6	1.4
Sn	1	2	1	<1	<1	1	1	2	<1	2	2	1	<1
La	49.7	28.2	40.0	43.2	27.9	9.58	213	143	177	187	118	191	143
Ce	88	45	65	56	34	11	406	255	548	356	229	584	279
Pr	7.93	4.24	5.99	4.23	2.54	0.80	40.9	26.4	40.6	33.2	24.0	42.8	30.4
Nd	32.3	14.1	23.5	14.3	8.53	2.57	151	92.4	141	125	82.3	154	106
Sm	6.15	2.36	4.28	1.85	1.10	0.33	31.0	19.0	27.9	25.1	15.9	29.5	18.0
Eu	1.852	0.798	1.091	0.974	1.003	1.090	1.954	1.655	1.568	1.866	1.660	1.606	1.650
Gd	4.88	2.16	3.48	1.46	0.80	0.22	24.9	20.5	25.2	19.7	15.5	25.5	15.2
Tb	0.70	0.31	0.53	0.19	0.10	0.03	4.55	3.76	4.36	3.01	2.80	4.38	2.17
Dy	3.31	1.70	2.75	0.81	0.42	0.07	23.5	23.2	25.8	15.6	18.4	25.5	13.4
Ho	0.57	0.38	0.54	0.14	0.08	0.01	4.00	5.37	5.64	3.04	4.44	5.40	3.26
Er	1.54	1.08	1.51	0.40	0.21	0.05	10.4	16.9	15.8	8.9	14.1	16.5	10.3
Tm	0.177	0.172	0.211	0.047	0.024	<0.005	1.451	2.984	2.426	1.314	2.538	2.544	1.638
Yb	0.94	1.02	1.20	0.28	0.18	0.05	7.98	18.4	13.8	7.87	16.0	14.5	9.57
Lu	0.133	0.180	0.167	0.048	0.036	0.010	1.115	2.853	1.991	1.092	2.619	2.072	1.410
Hf	6.5	2.8	5.0	2.9	3.3	0.1	12	8.6	10	7.9	10	9.4	8.3
Ta	0.3	0.4	0.5	0.1	<0.1	0.1	0.5	0.4	1.1	1.0	0.3	1.2	0.2
Pb	14	6	20	29	17	36	104	52	42	123	23	30	34
Th	1.54	1.72	2.42	1.24	0.66	0.06	147	68.3	204	122	71.1	200	105
U	0.36	0.22	1.40	0.16	0.22	<0.05	6.94	12.2	10.2	13.8	9.92	15.9	9.18

Table 1 (continued).

Sample No.	127	282-2	301	282-1	117	61-2	61-1	151	601	228	208	289
Rock Facies	*garnet-rich garnet felsic gneiss*				*garnet-sillimanite gneiss*			*quartz- free mafic gneiss*				
Mineral Assemblage	Grt, Meso Pl, Qtz Zm, Ilm, Rt	Grt, Meso Pl, Qtz Zm, Ilm, Rt	Grt, Meso Pl, Qtz Zm,Mo,Ilm, Rt	Grt, Meso Pl, Qtz Zm, Ilm, Rt	Grt, Sil, Spl Bt, Zm, Ilm Qtz, Pl	Grt, Sil, Spl Zm, Ilm Qtz, Pl	Grt, Sil, Spl Zm, Ilm Qtz, Pl	Cpx, Opx Pl, Ap Ilm, Bt	Opx, Cpx Pl Ilm, Mag	Opx, Cpx Pl Ilm, Mag	Opx, Cpx Pl Ilm	Opx, Cpx Pl, Ap Ilm, Mag
(wt.%)												
SiO2	68.98	70.69	72.64	75.80	53.15	54.34	58.58	47.21	48.38	48.68	48.84	49.08
TiO2	0.53	0.51	0.52	0.36	1.29	1.15	0.96	1.07	1.18	0.96	0.73	0.86
Al2O3	13.20	13.59	13.15	11.85	22.87	20.12	17.42	13.58	12.96	13.14	14.92	14.15
Fe2O3	8.17	7.07	5.35	5.01	15.02	11.46	11.08	14.32	15.85	14.41	13.54	13.62
MnO	0.08	0.08	0.06	0.06	0.07	0.12	0.12	0.20	0.21	0.19	0.16	0.18
MgO	2.73	2.44	1.91	1.76	4.11	3.92	4.10	7.99	8.13	7.28	9.65	8.43
CaO	1.62	1.92	1.93	1.89	0.75	4.96	4.25	13.18	10.26	11.38	10.78	11.50
Na2O	1.64	2.01	1.87	1.96	0.00	2.28	1.70	1.47	1.90	1.71	1.06	1.56
K2O	2.38	1.91	2.72	1.64	1.23	0.52	0.52	0.15	0.15	0.48	0.26	0.43
P2O5	-	0.01	0.01	-	-	0.06	0.05	0.06	0.03	0.03	0.04	0.02
Total	99.33	100.23	100.16	100.34	98.48	98.94	98.79	99.23	99.05	98.26	99.97	99.83
(ppm)												
Ba	692.5	417.7	878.5	338.3	287.8	340.2	318.9	14.3	-	32.0	21.8	10.9
Co	24.0	17.2	17.0	13.2	59.3	61.2	60.8	55.9	58.4	56.4	55.9	53.2
Cr	166.9	134.2	100.0	98.8	682.7	266.2	202.8	305.6	207.7	156.4	350.9	281.5
Cu	49.9	21.3	21.6	18.1	34.5	65.0	55.2	65.0	110.4	86.6	105.9	76.5
Nb	29.3	13.6	12.3	7.4	18.8	20.3	14.8	4.0	8.4	14.6	5.8	2.3
Ni	70.5	9.9	41.6	9.4	64.1	126.9	133.7	147.8	111.2	117.2	183.3	140.4
Rb	67.4	46.6	76.8	39.3	45.8	14.2	15.9	4.1	1.9	19.0	4.9	8.3
Sr	129.4	171.4	223.7	165.3	41.4	86.9	73.9	115.8	88.9	82.7	80.2	89.7
V	89.6	90.0	72.1	61.4	338.1	255.5	230.5	292.0	301.5	277.0	280.6	256.4
Y	53.6	35.1	31.6	29.9	65.9	70.0	56.5	23.6	36.1	35.5	32.9	21.8
Zn	62.5	41.4	44.4	33.9	132.5	124.2	37.8	94.1	120.3	103.5	110.7	102.9
Zr	208.4	167.9	193.3	137.8	225.8	259.8	217.1	43.2	40.0	41.8	23.9	37.3
Ga	15	14	19	13	31	22	25	15	17	16	17	15
Ge	1.4	1.3	1.3	1.1	4.1	1.9	2.5	1.6	1.3	1.7	1.1	1.4
Sn	<1	<1	<1	<1	<1	<1	<1	2	2	4	1	2
La	29.8	39.8	46.3	39.0	37.7	35.0	53.0	2.87	4.81	5.93	3.58	3.53
Ce	49	66	81	67	70	68	102	8.5	12	15	10	9.1
Pr	4.70	6.38	7.75	6.37	7.46	7.58	11.1	1.29	1.82	2.00	1.48	1.34
Nd	16.7	23.4	27.5	23.0	30.4	29.4	42.6	7.78	8.94	10.8	7.84	7.31
Sm	3.56	4.76	4.96	3.77	7.87	6.95	9.23	2.67	2.86	3.59	2.96	2.55
Eu	1.302	1.308	1.565	1.323	1.429	1.651	2.383	0.987	0.940	0.960	0.684	0.816
Gd	4.86	5.15	4.02	3.87	8.22	7.98	10.6	3.38	3.73	4.51	3.75	3.42
Tb	1.16	0.94	0.78	0.72	1.52	1.52	1.90	0.66	0.83	0.96	0.87	0.67
Dy	8.07	5.50	4.77	4.36	10.5	9.64	12.1	4.04	5.66	6.05	5.93	4.12
Ho	1.83	1.16	1.00	0.92	2.52	2.13	2.72	0.87	1.37	1.27	1.23	0.85
Er	5.28	3.42	3.14	2.78	7.61	5.91	7.72	2.50	4.24	3.59	3.27	2.37
Tm	0.838	0.514	0.470	0.412	1.241	0.935	1.242	0.407	0.648	0.574	0.472	0.359
Yb	4.74	3.21	3.00	2.58	7.47	5.44	7.09	2.46	4.04	3.30	2.56	2.29
Lu	0.699	0.468	0.446	0.388	1.107	0.791	1.022	0.353	0.620	0.456	0.362	0.328
Hf	5.8	3.8	5.1	3.1	6.0	5.7	7.2	1.1	1.3	1.2	0.9	0.9
Ta	3.2	1.1	0.7	0.8	1.7	1.1	2.4	0.1	0.3	0.8	0.2	0.2
Pb	13	32	40	28	<5	6	8	<5	<5	<5	<5	<5
Th	4.34	2.55	13.5	2.16	11.0	1.68	6.25	0.06	1.10	0.20	0.22	<0.05
U	0.87	0.36	0.67	0.34	0.50	0.46	0.90	<0.05	0.09	<0.05	<0.05	<0.05

Table 1 (continued).

Sample No.	298	154	235	503	501	508	507	502	556	551	553
Rock Facies	*quartz- bearing mafic gneiss*			*phlogopite-bearing meta-ultramafic rocks*					*phlogopite-free meta-ultramafic rocks*		
Mineral Assemblage	Opx, Cpx Pl, Qtz Ilm, Mag	Opx, Cpx Pl, Qtz Ilm	Cpx, Opx Pl, Qtz Ilm, Bt	Ol Spl, Phl	Ol, Opx Spl, Phl	Ol, Opx, Cpx, Phl, Spl	Ol, Opx, Cpx, Spl, Phl	Ol, Opx, Cpx, Spl, Phl	Ol, Opx, Spl	Ol, Opx, Cpx, Spl	Ol, Opx, Spl
(wt.%)											
SiO2	50.12	50.70	51.99	40.40	42.01	48.42	49.08	50.64	45.75	46.20	47.97
TiO2	2.67	0.63	0.65	0.08	0.13	0.30	0.25	0.16	0.07	0.15	0.08
Al2O3	13.18	11.37	15.19	0.98	2.00	7.15	6.38	3.39	2.48	2.87	2.54
Fe2O3	18.81	12.48	10.19	9.45	8.11	10.63	8.86	7.41	7.44	7.35	7.44
MnO	0.17	0.19	0.12	0.13	0.11	0.16	0.13	0.09	0.12	0.12	0.13
MgO	4.93	11.96	7.59	43.76	44.33	26.16	25.79	31.23	40.79	41.34	40.78
CaO	5.83	11.05	9.95	1.52	2.06	4.55	7.78	4.25	0.93	0.81	0.69
Na2O	2.16	1.65	2.52	0.09	0.14	0.14	0.15	0.20	0.06	0.03	0.33
K2O	0.65	0.31	0.59	0.25	0.04	-	0.03	0.02	-	0.04	-
P2O5	0.53	0.03	0.10	0.01	0.02	0.01	0.01	0.01	0.01	0.01	0.01
Total	99.04	100.36	98.88	96.67	98.95	97.51	98.46	97.41	97.64	98.92	99.96
(ppm)											
Ba	308.8	63.6	220.5	22.0	14.4	13.2	16.6	19.8	15.6	4.2	21.5
Co	52.9	59.9	44.4	105.4	99.0	72.3	63.4	57.0	84.6	82.9	80.9
Cr	96.1	856.6	344.4	1711	2031	2748	2446	2043	2118	1593	1888
Cu	129.0	57.2	58.7	-	1.5	-	1.2	4.4	-	-	-
Nb	24.2	4.0	12.7	1.0	4.1	1.7	2.9	1.6	1.1	3.8	0.3
Ni	88.1	307.5	136.1	2917	3043	979.5	983.1	1472	2266	2376	2180
Rb	5.3	28.6	8.6	8.2	-	-	2.1	-	-	2.9	0.2
Sr	168.9	146.0	128.0	6.6	9.8	4.9	6.4	11.7	4.5	6.1	3.5
V	362.7	151.6	175.6	-	36.6	128.0	120.6	68.1	30.2	39.7	35.7
Y	44.7	11.1	18.6	3.1	4.6	11.3	12.5	18.9	3.7	10.6	3.0
Zn	148.7	101.9	86.0	48.3	41.0	95.3	71.3	520.1	41.8	41.2	35.7
Zr	111.4	67.0	41.4	8.8	18.2	38.0	34.5	39.6	13.0	23.9	9.3
Ga	27	13	17	2	2	8	6	5	3	3	3
Ge	1.8	1.3	1.5	0.8	<0.5	1.2	1.4	0.9	0.9	1.0	1.1
Sn	3	<1	2	<1	3	<1	<1	3	2	2	1
La	28.0	9.97	23.7	0.82	3.98	2.99	7.65	7.08	0.72	2.17	0.39
Ce	52	25	43	1.6	9.3	8.9	23	13	2.7	6.8	1.1
Pr	6.08	3.13	4.33	0.20	1.02	1.17	2.67	1.73	0.41	0.97	0.14
Nd	26.3	13.2	17.2	0.80	3.54	5.20	9.93	7.90	1.66	4.76	0.60
Sm	6.47	3.04	3.63	0.23	0.73	1.25	1.99	2.05	0.41	1.43	0.21
Eu	1.813	0.954	0.874	0.092	0.198	0.279	0.437	0.463	0.074	0.191	0.036
Gd	6.60	3.05	3.37	0.29	0.65	1.45	1.98	2.33	0.44	1.61	0.24
Tb	1.25	0.53	0.60	0.06	0.11	0.27	0.33	0.47	0.08	0.30	0.06
Dy	7.42	3.16	3.41	0.37	0.65	1.70	1.99	3.10	0.54	1.80	0.41
Ho	1.52	0.65	0.67	0.08	0.14	0.37	0.41	0.66	0.12	0.38	0.10
Er	4.45	1.77	1.87	0.22	0.40	1.04	1.20	1.79	0.39	0.98	0.35
Tm	0.654	0.261	0.285	0.037	0.057	0.167	0.177	0.265	0.063	0.152	0.056
Yb	4.05	1.59	1.67	0.21	0.37	0.99	1.11	1.58	0.44	0.80	0.38
Lu	0.609	0.221	0.240	0.034	0.057	0.149	0.162	0.218	0.070	0.111	0.067
Hf	3.1	1.9	1.0	0.2	0.4	1.0	0.9	1.2	0.4	0.8	0.3
Ta	1.1	0.2	0.8	<0.1	0.3	0.2	0.2	0.1	<0.1	0.2	<0.1
Pb	9	<5	12	<5	<5	<5	<5	<5	<5	<5	<5
Th	5.73	0.65	3.48	0.37	0.15	1.99	3.63	2.70	0.06	0.50	0.16
U	0.73	0.11	0.42	0.16	<0.05	0.18	0.33	1.07	<0.05	0.14	<0.05

Fe_2O_3* means total iron as Fe_2O_3.
Abbreviations: Bt=biotite, Cpx=clinopyroxene, Grt=garnet, Ilm=ilmenite, Mag=magnetite, Meso=mesoperthite, Ol=olivine, Opx=orthopyroxene, Phl=phlogopite, Pl=plagioclase, Qtz=quartz, Rt=rutile, Spl=spinel, Xe=xenotime, Zrn=zircon.

rocks were analyzed with inductively coupled plasma mass spectrometry (ICP-MS) at Activation Laboratories Ltd. The localities of analyzed samples are given in Figs. 2 and 3, and their mineral assemblages and bulk rock analyses are listed in Table 1.

Inasmuch as some elements such as large iron lithophile elements (*e.g.*, K, Rb, Sr and Ba) have been known to be mobile during low- to medium-grade metamorphism, the primary compositions of the low- to medium-grade metamorphic rocks may have been masked (*e.g.*, TARNEY and WINDLEY, 1977; CONDIE, 1981). However, SHERATON (1984) suggested that the chemical modification in metamorphic rocks is not effective under the high-grade metamorphism of the Napier Complex. We, therefore, assume that the chemical features described hereafter are useful in the characterization of original rocks, except for some REEs such as La and Eu in meta-ultramafic rocks, as stated later.

3.1. Major and minor elements

The variations of major and minor elements against the SiO_2 content are shown in Figs. 7 and 8, respectively. The orthopyroxene felsic gneisses range in SiO_2 from 64 to 73 wt%. Although most of their major and minor element contents are rather scattered against the SiO_2 content, it appears that, with increasing SiO_2 content, the majority of other major elements (except K_2O) and some minor elements such as Ni, Co, Zn, Zr, Nb, Y and V decrease, while the K_2O, Sr and Ba contents increase.

Both garnet felsic gneiss I and II have similar SiO_2 contents ranging from 67 to 77 wt%, but the former is poor in TiO_2, Fe_2O_3*, MgO, MnO, CaO, Cr, Co, Zn, V, Sr and Cu, and rich in Al_2O_3, Na_2O, K_2O, P_2O_5, Y and Rb, as compared with the latter. Both types show decreasing variations in TiO_2, Al_2O_3, Fe_2O_3*, MgO, Co, Zn, Y and Rb with increasing SiO_2 content, but the decreasing slopes are slightly different between the two types. Furthermore, the garnet felsic gneiss II shows distinctive decreases in Cr and V with increasing SiO_2 content.

The garnet-sillimanite gneisses range in SiO_2 from 52 to 59 wt%. Of particular interest of the garnet-sillimanite gneisses is the highest Al_2O_3 content among the analyzed rocks, and further some of the garnet-sillimanite gneisses are characterized by strong depletion in CaO, Na_2O and P_2O_5. Systematic decreases in TiO_2, Al_2O_3, Fe_2O_3*, Co, Zn, Nb, Y and V with increasing SiO_2 content are distinctive in the garnet-sillimanite gneisses.

The SiO_2 contents of the quartz-free mafic gneiss vary from 47 to 49 wt%, and those of the quartz-bearing variety from 50 to 52 wt%. Other major and minor elements are either constant or scattered in the quartz-free type, while in the quartz-bearing type these elements show wide ranges without systematic trends against the SiO_2 content. No. 298 of the quartz-bearing mafic gneiss with 50.12 wt% SiO_2 is considerably enriched in TiO_2, P_2O_5 and Nb, and depleted in MgO, CaO and Cr, as compared with other mafic gneisses. Relatively enriched features in Co (44–60 ppm), Cr (156–857 ppm), and Ni (117–307 ppm) in the mafic gneisses, except the sample of No. 298, are characteristic of the Archaean mafic rocks (CONDIE, 1985).

The meta-ultramafic rocks range in SiO_2 from 43 to 48 wt% for the phlogopite-free type, and from 40 to 50 wt% for the phlogopite-bearing type. The phlogopite-free type is enriched in MgO, Ni and Co, and depleted in Al_2O_3, CaO and V, as compared with the phlogopite-bearing type. With increasing SiO_2 content, the systematic increases in Al_2O_3, CaO, Cr, V and decreases in MgO and Ni are most characteristic of the phlogopite-

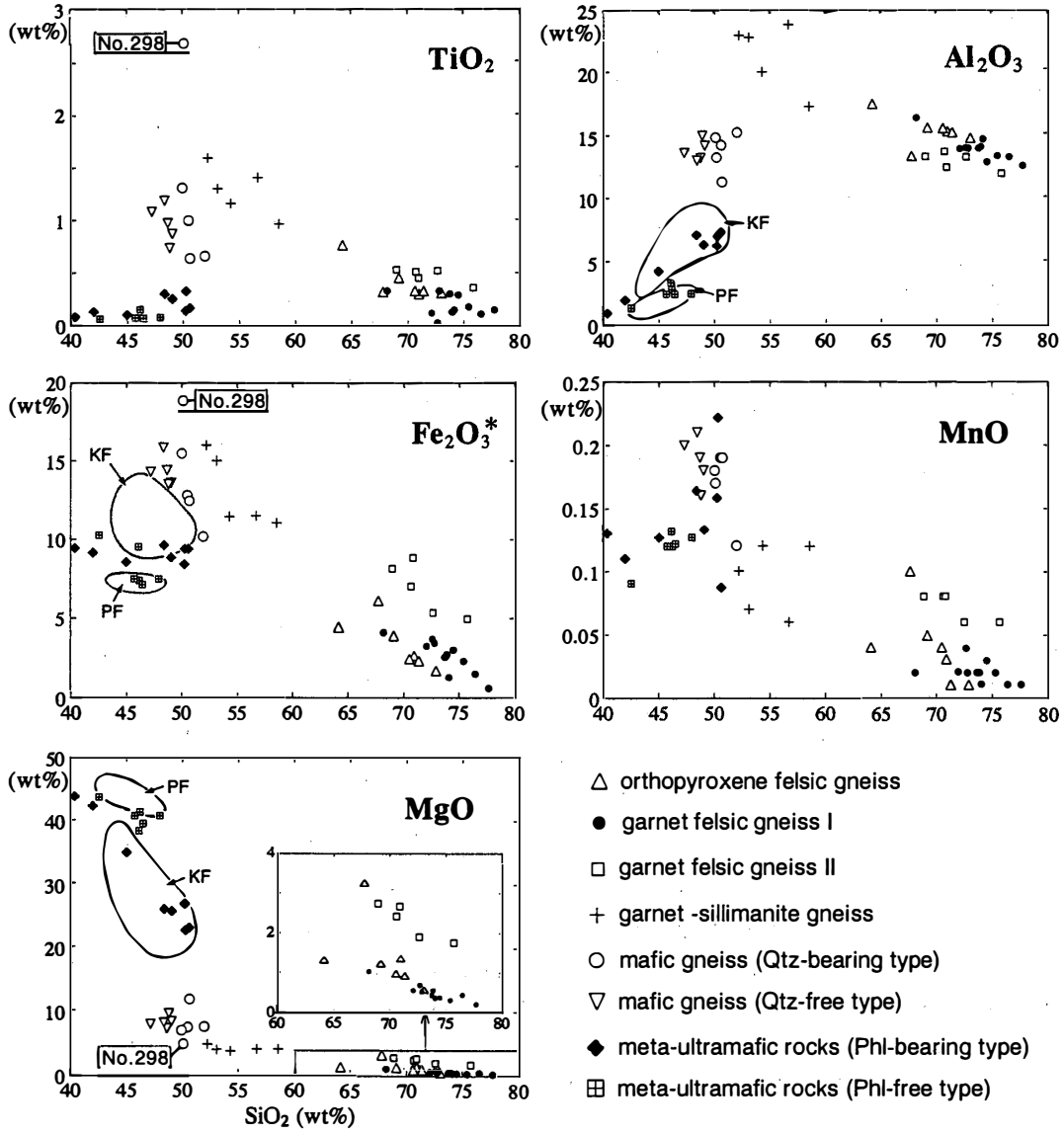

Fig. 7. Variation diagrams of major elements against the SiO_2 content for the metamorphic rocks from the Mt. Riiser-Larsen area. KF and PF mean the compositional fields of komatiite (Munro-type komatiites of 2.7 Ga) and peridotite (after HERZBERG (1992) and TAKAHASHI (1990)), respectively.

bearing type. These elements except for Cr of the phlogopite-free type also vary in a similar sense to the phlogopite-bearing type, but their slopes are more gentle. The Cr content seems to decrease in the phlogopite-free type but increase in the phlogopite-bearing type, with increasing SiO_2 content.

3.2. Rare earth elements

The chondrite-normalized patterns of REEs are illustrated in Fig. 9. The orthopyroxene felsic gneisses have a wide range of REE concentrations from 10–100 times chondrite values in light REE (LREE) to 0.2–10 times chondrite values in heavy REE (HREE). This seems to be antithetically related to the SiO_2 content, namely, the REE

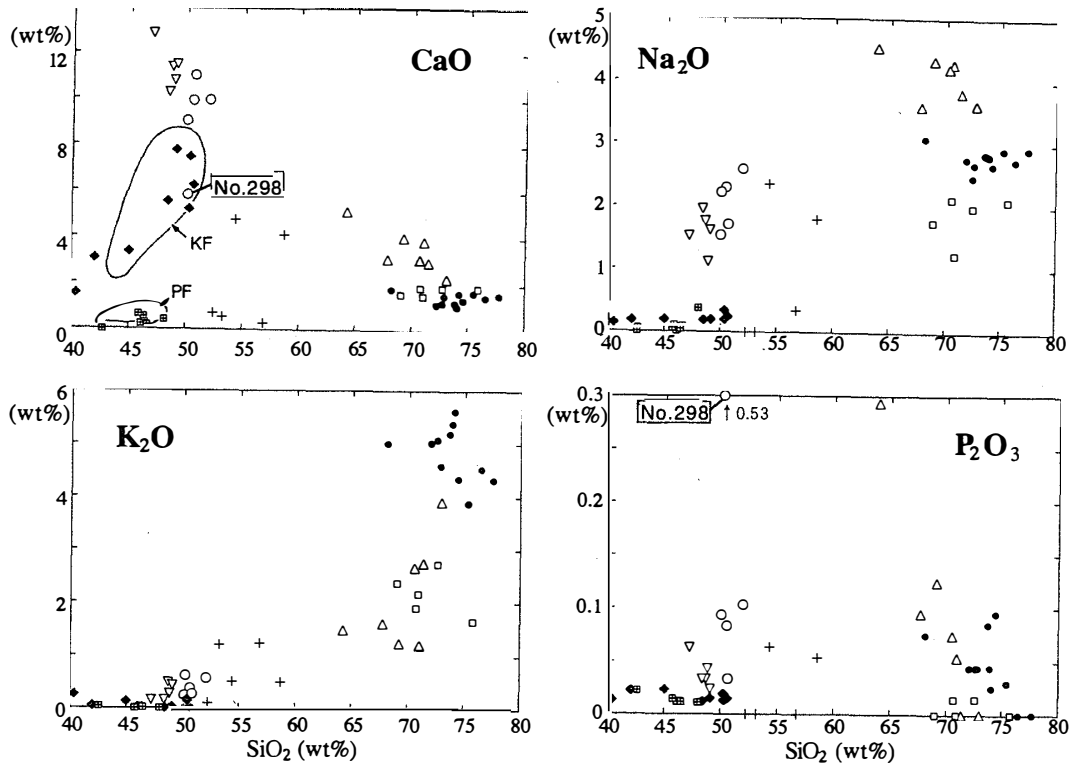

Fig. 7 (continued).

concentrations except Eu decrease with increasing SiO_2 content. The positive Eu anomalies are characteristic of the orthopyroxene felsic gneisses. The degree of the Eu anomaly becomes high with increasing the SiO_2 content, but the Eu concentrations are relatively constant. The modal proportion of feldspar is relatively constant (60–70%) among the analyzed orthopyroxene felsic gneisses, but the accessory minerals such as zircon, monazite, apatite, magnetite and ilmenite decrease in modal proportion with increasing SiO_2 content. Thus, the changes of REE concentrations and Eu anomaly described above must be related to the modal proportion of REE-bearing minerals such as zircon, monazite and apatite, which will be further discussed in a later section.

The REE patterns of the garnet felsic gneiss I are relatively flat in HREE but enriched in LREE, with negative Eu anomaly. The high REE concentrations are also characteristic of this type, which may be attributed to relatively high abundances of accessory minerals such as apatite, xenotime, zircon and monazite. Garnet felsic gneiss II has lower REE concentrations than the type I variety, and displays LREE-enriched and flat HREE patterns without the Eu anomaly.

The garnet-sillimanite gneisses show the LREE-enriched and flat HREE patterns with slightly negative Eu anomalies. Although the REE concentrations are slightly higher in the garnet-sillimanite gneiss than in the garnet felsic gneiss II, their REE patterns except Eu are very similar to each other. As the Eu concentration is nearly equal between these two gneisses, the difference of other REE concentrations may be due to the lower abundance of accessory minerals such as zircon in the garnet felsic gneiss II than in the garnet-sillimanite gneiss.

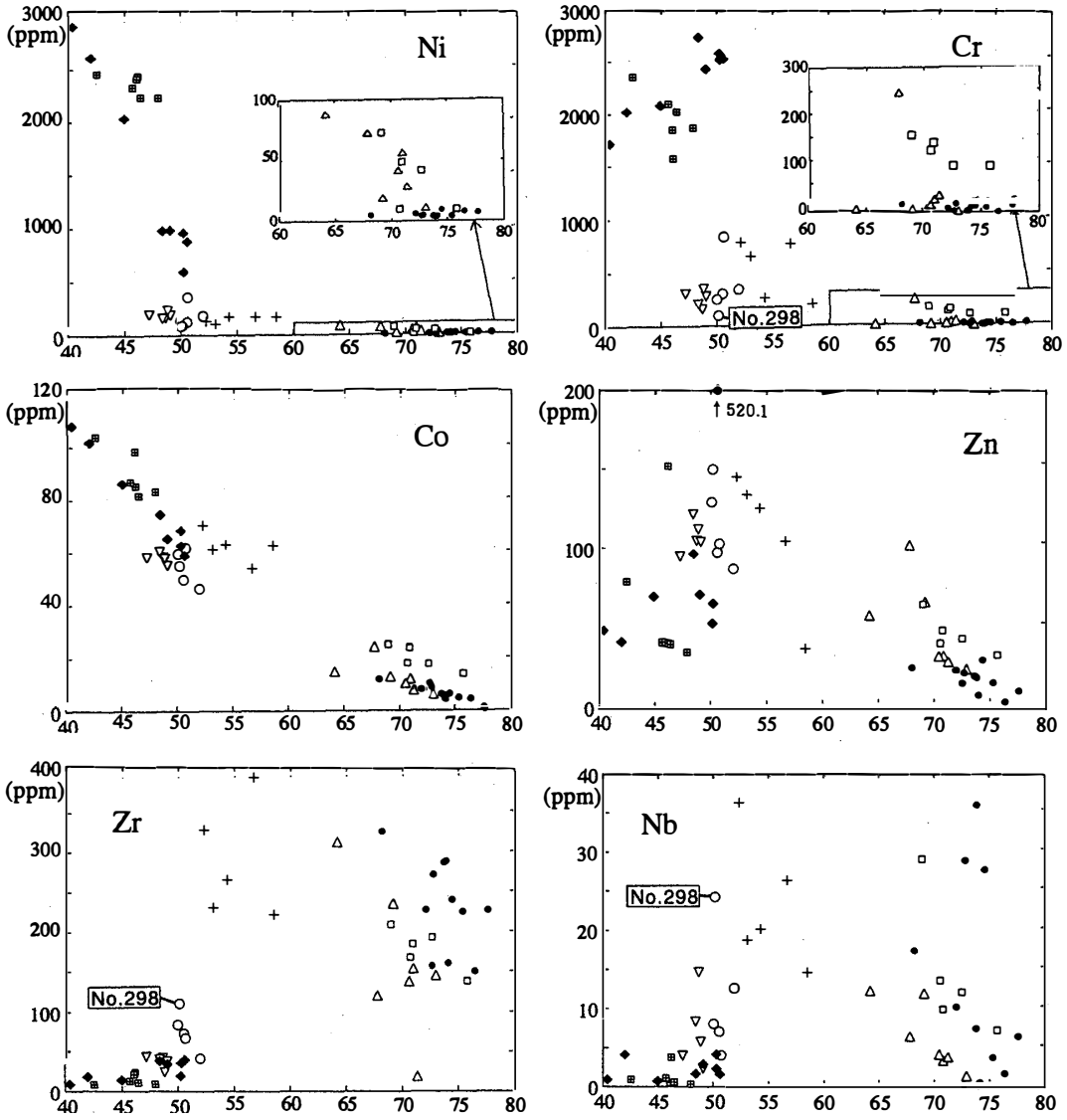

Fig. 8. Variation diagrams of minor elements against the SiO_2 content for the metamorphic rocks from the Mt. Riiser-Larsen area. Symbols are the same as in Fig. 7.

The quartz-bearing type of the mafic gneisses shows the LREE-enriched pattern, while the quartz-free type has the flat or slightly LREE-depleted pattern; both types have the flat or slightly HREE-depleted pattern. The Eu anomaly is distinct in the quartz-free type, but not so clear in the quartz-bearing type.

Very low REE concentrations are most characteristic of the meta-ultramafic rocks, ranging from 1 to 40 times chondrite values. The phlogopite-bearing type shows the slightly LREE-enriched and flat HREE pattern, while the REE pattern of the phlogopite-free type is rather flat. Some of the analyzed meta-ultramafic rocks have a weak positive or negative Eu anomaly and La depletion. SUN and NESBITT (1978) and LAHAYE and ARNDT (1996) have suggested that the En and/or La concentration of ultramafic or komatiitic rocks has been slightly but significantly mobilized during the low-grade alteration, although, as suggested by ROLLINSON (1999), in samples with REE concentrations

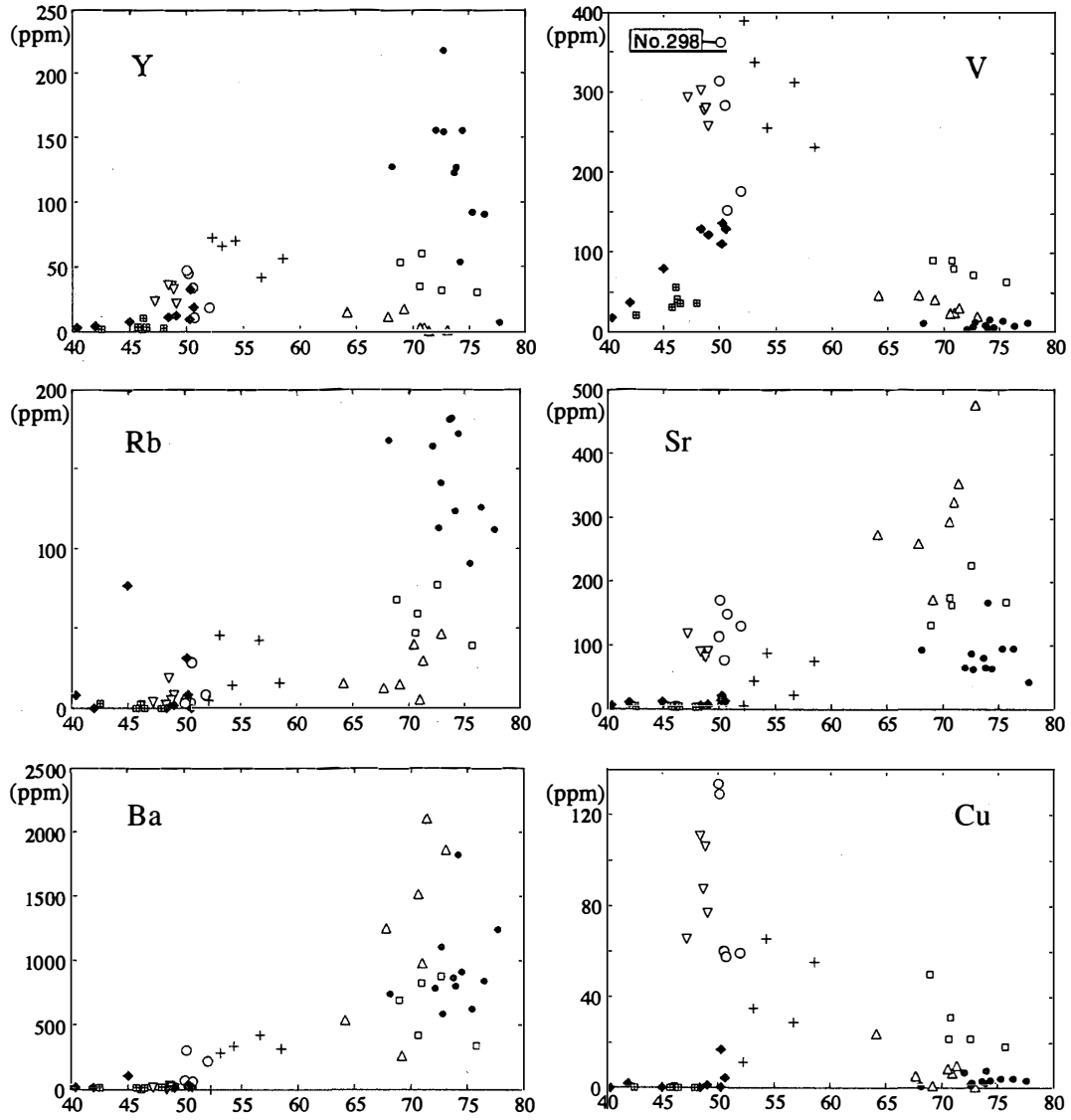

Fig. 8 (continued).

less than 2–3 times chondrite values, the analytical precision in this study was not sufficiently good to substantiate Eu anomaly and/or La depletion.

4. Possible Precursors of UHT Metamorphic Rocks

One of the important problems of the Napier complex maybe whether its precursor is igneous or sedimentary in origin, which is assessed as follows based on the geochemical constraints mentioned above.

First, we notice the unusual bulk rock chemistry of the garnet-sillimanite gneiss, especially its high Al_2O_3 content. No major or minor element increases with increasing SiO_2 content (Figs. 7 and 8). These chemical features cannot be derived by differentiation from any kind of igneous rock. As shown in Fig. 10, the calculation of A (Al_2O_3+Fe_2O_3−Na_2O−K_2O)−C(CaO)−F(FeO+MgO+MnO) molecular components indicates the

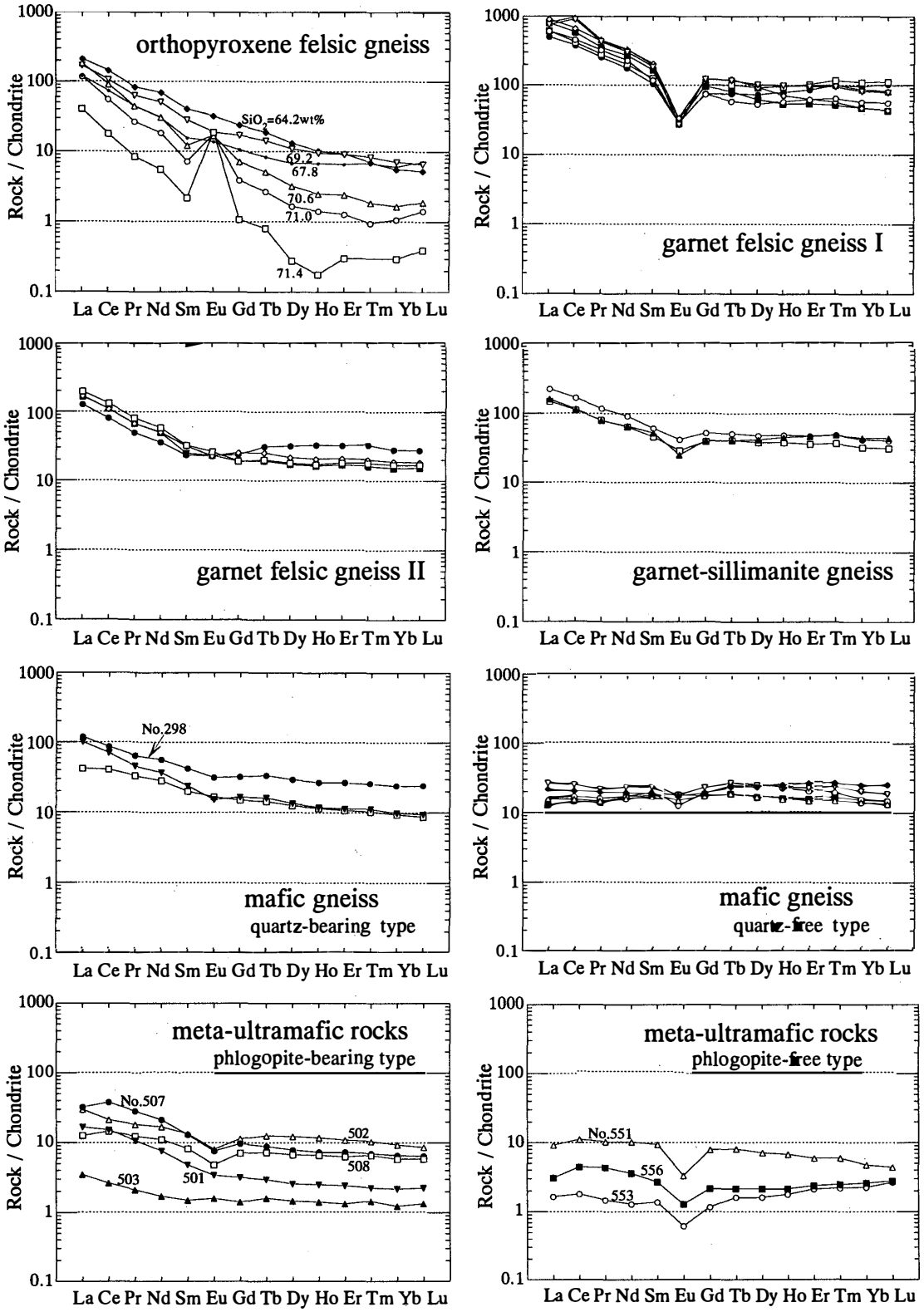

Fig. 9. Rare earth element abundances normalized to chondrite (after SUN and MCDONOUGH, 1989) for metamorphic rocks from the Mt. Riiser-Larsen area.

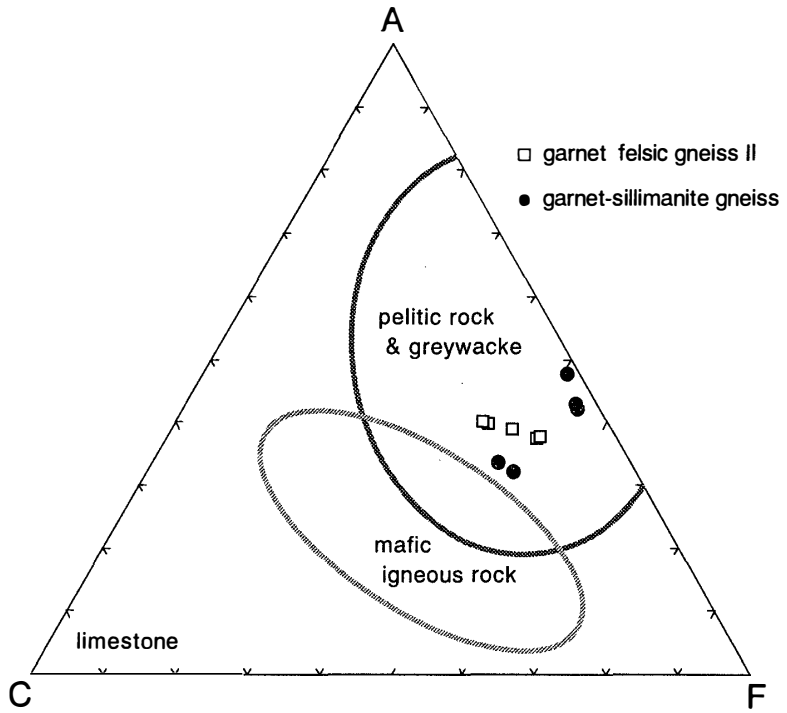

Fig. 10. ACF diagram for garnet felsic gneiss II and garnet-sillimanite gneiss. The areas of common metamorphic rocks are delineated as modified after MIYASHIRO (1994). The FeO/Fe_2O_3 molecular ratio is estimated based on the wet chemical analyses of SHERATON et al. (1987), namely, it is 0.64 for garnet felsic gneiss II and 0.92 for garnet-sillimanite gneiss.

analyzed garnet-sillimanite gneisses to be poor in the C component, and to have an affinity with the sedimentary rocks (pelitic rocks) in the sense described by MIYASHIRO (1994). This implies that the garnet-sillimanite gneisses have been derived from sedimentary rocks such as mudstone.

To test the chemical features of original rocks of the garnet felsic gneisses, we use the discriminant functions for protoliths between silicic volcanics and sandstones (DF3 and DF4) derived from SHAW (1972). These equations are as follows:

$$DF3=10.44-0.21SiO_2-0.32Fe_2O_3{}^*(\text{total Fe as } Fe_2O_3)$$
$$-0.98MgO+0.55CaO+1.46Na_2O+0.54K_2O,$$

and

$$DF4=-39.59+0.42SiO_2+0.30Fe_2O_3{}^*+0.89MgO+1.53CaO+0.58Na_2O$$
$$+2.07K_2O-0.037Cr+0.005V-0.027Ni-0.001Sr.$$

Both of the DF values are generally positive for igneous rocks and negative for sedimentary rocks. The calculation indicates that the DF values are positive for the garnet felsic gneiss I (DF3 ranging from 0.25 to 2.02, and DF4 from 4.71 to 6.93) and negative for the garnet felsic gneiss II (DF3 ranging from −4.76 to −3.13, and DF4 from −5.14 to −0.80). This may suggest that the garnet felsic gneiss I and II are igneous and sedimentary in origin, respectively.

The sedimentary origin for the garnet felsic gneiss II is also suggestive in the ACF diagram (Fig. 10). Furthermore, the similar REE patterns between the garnet-sillimanite

gneiss and garnet felsic gneiss II (Fig. 9) seem to support their similar origin. The field occurrence of the garnet felsic gneiss II, such as alternation with the garnet-sillimanite gneiss, further supports their sedimentary origin, probably similar to alternation of mudstone and sandstone.

On the other hand, the garnet felsic gneiss I has acidic composition; the calculation of CIPW norm components indicates that they fall in the granite field with the systematic trend toward the Or component (Fig. 11). It is, therefore, likely that the garnet felsic gneiss I has been derived from the igneous (granitic) rocks.

As suggested by SHERATON *et al.* (1987), we also assume that the other rock types have been derived from igneous rocks. If this is the case, the observed compositional variations such as the decreases in TiO_2, Fe_2O_3*, MgO, CaO, P_2O_5, Zr and V with increasing SiO_2 content in the orthopyroxene felsic gneisses (Figs. 7 and 8) may represent igneous differentiation trends mainly controlled by fractionation of amphibole (and/or clinopyroxene), Fe-Ti oxide and accessories such as zircon, apatite and possible monazite. As the HREEs are strongly partitioned into amphibole (MARTIN, 1987) and the LREEs into apatite and monazite (CHANG *et al.*, 1998), the decreases in REE concentrations and the increase in the degree of Eu anomaly with increasing SiO_2 content observed in the orthopyroxene felsic gneisses (Fig. 9) may also be explained by fractionation of amphibole and these accessory minerals. On the $(Na_2O+K_2O)-SiO_2$ diagram (Fig. 12), the orthopyroxene felsic gneisses are plotted in the non-alkaline field, and have a calc-alkaline affinity on the AFM diagram (Fig. 13). Furthermore, on the normative An-Ab-Or diagram (Fig. 11), the orthopyroxene felsic gneisses fall in the field of tonalite to

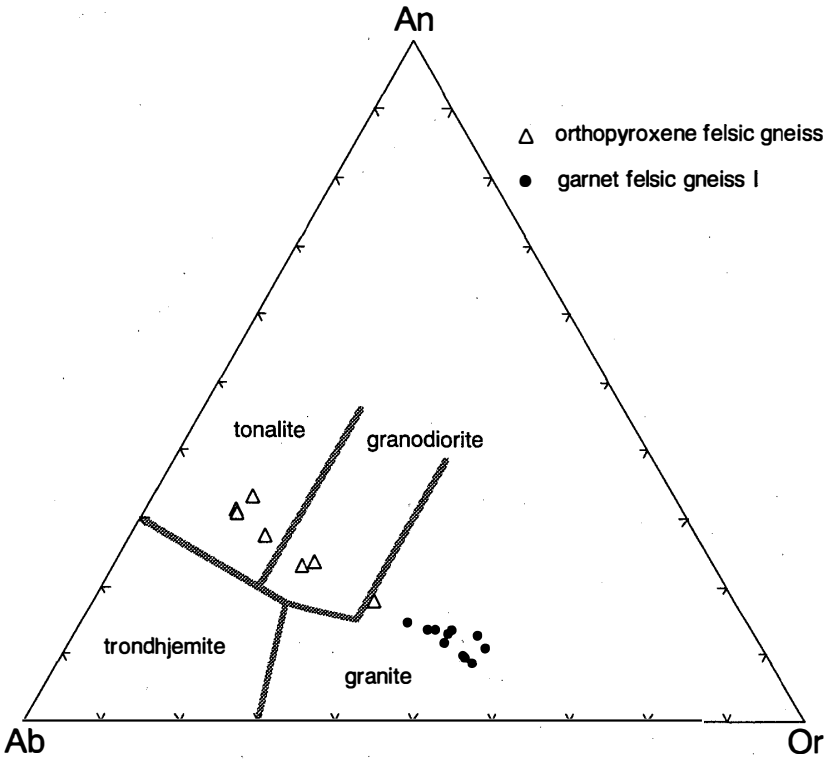

Fig. 11. Normative An-Ab-Or diagram (after BARKER, 1979) for the garnet felsic gneiss I and orthopyroxene felsic gneiss.

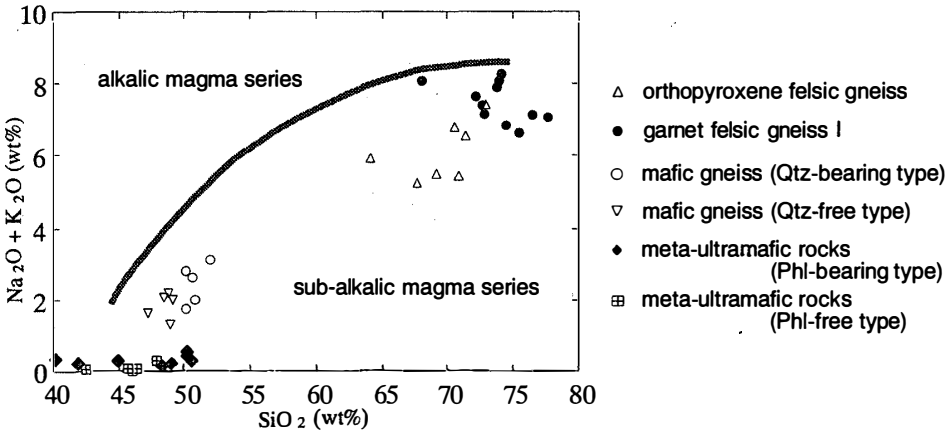

Fig. 12. Alkali-silica diagram for the metamorphic rocks derived from igneous lithology. The dividing curved line between alkalic and sub-alkalic magma series is after MIYASHIRO (1978).

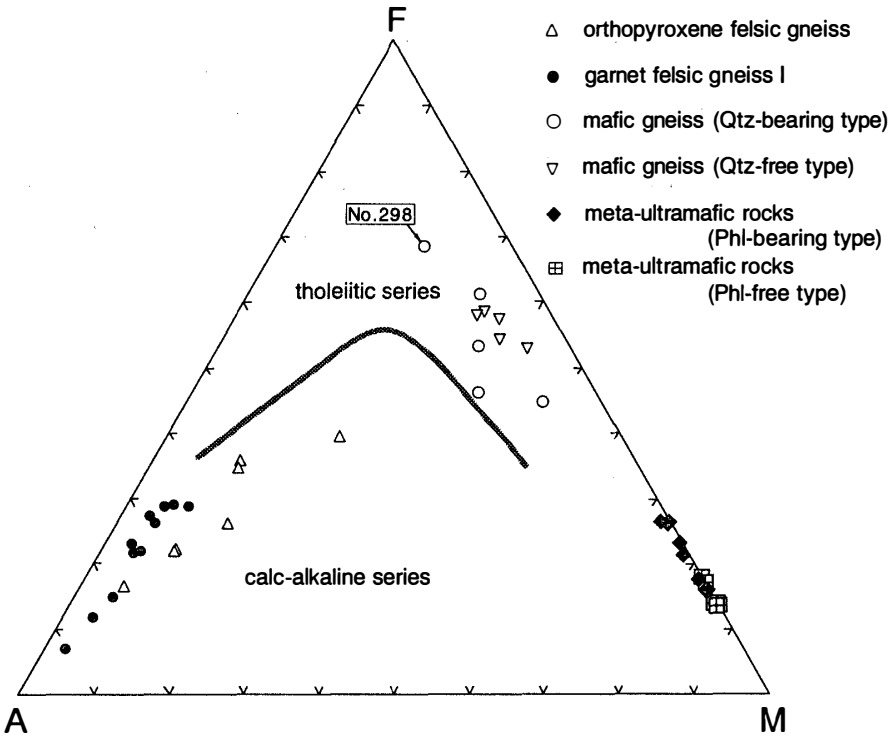

Fig. 13. AFM diagram for the metamorphic rocks derived from igneous lithology. The dividing curved line between tholeiitic and calc-alkaline magma series is after IRVINE and BARAGAR (1971).

granodiorite. In this connection, the chondrite normalized $(La/Yb)_N$-Yb_N relations (Fig. 14) indicate that the orthopyroxene felsic gneisses have an affinity with the Archaean TTG (tonalite-trondhjemite-granodiorite) (LUAIS and HAWKESWORTH, 1994). It is, therefore, likely that the orthopyroxene felsic gneisses have been derived from tonalitic to granodioritic precursors with the Archaean TTG signature.

Both the quartz-free and -bearing mafic gneisses are plotted in the non-alkaline

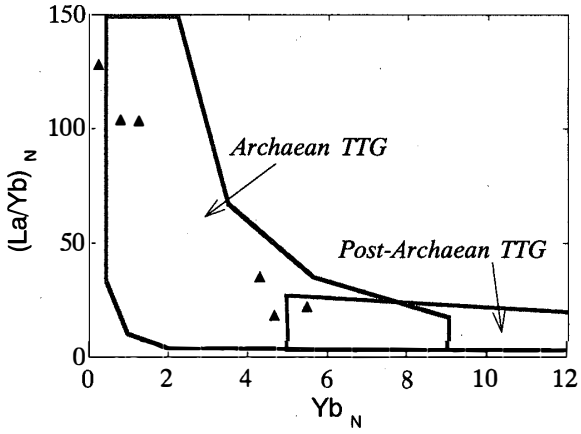

Fig. 14. $(La/Yb)_N$ versus Yb_N diagram for the orthopyroxene felsic gneisses. Fields of Archaean TTG and Post-Archaean TTG, and REE normalization are after LUAS *and* HAWKESWORTH *(1994).*

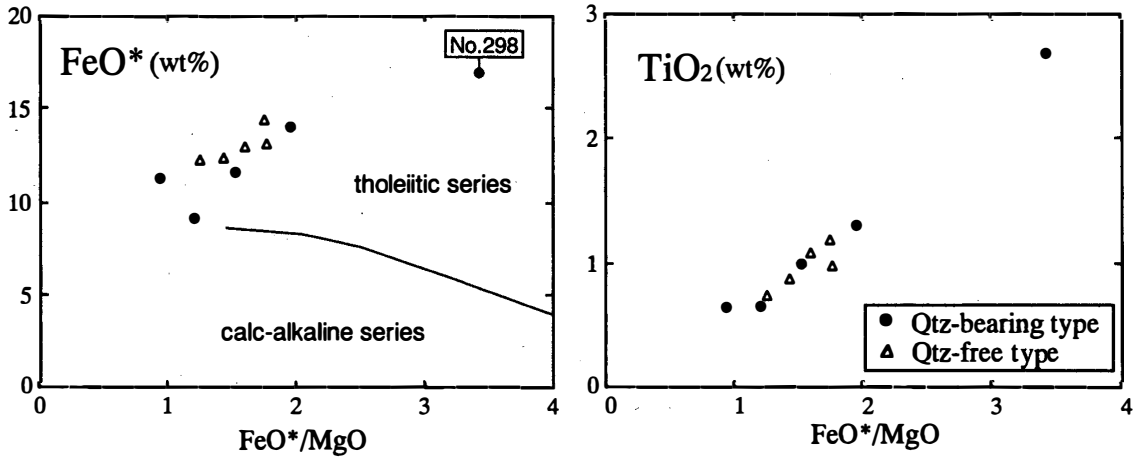

Fig. 15. FeO- and TiO_2-FeO*/MgO diagrams for the mafic gneisses. The dividing curved line between tholeiitic and calc-alkaline magma series is after* MIYASHIRO *(1974).*

basaltic field on the $(Na_2O+K_2O)+SiO_2$ diagram (Fig. 12). Although the majority of major and minor elements show no sign of systematic variation against the SiO_2 content (Figs. 7 and 8), on the AFM diagram (Fig. 13) they exhibit a tholeiitic differentiation trend, which is also indicated on the FeO*- and TiO_2-FeO*/MgO diagrams (Fig. 15). On these diagrams, it is clear that No. 298 of the quartz-bearing mafic gneiss is the most differentiated rock. These chemical features indicate that the mafic gneisses have been derived from the tholeiitic igneous suites. However, the LREE patterns are apparently different from each other (Fig. 9). As crystal fractionation of minerals common in tholeiitic rocks such as olivine, clinopyroxene and plagioclase are not able to significantly alter the LREE pattern (SUN and NESBITT, 1978), the difference in LREE patterns suggests that these two types of mafic gneisses cannot be derived from the same parental magma. It is rather possible that their source mantles have been different in LREE signature, namely, a LREE-enriched mantle for the quartz-bearing mafic gneiss and a LREE-depleted mantle for the quartz-free variety.

The petrogenetic relationship between basic (now represented by mafic gneiss) and felsic rocks (now represented by garnet felsic gneiss I and orthopyroxene felsic gneiss) is

one of the most significant problems in understanding the crustal evolution of the Archaean Napier Complex. Several processes have been proposed, such as partial melting of descending oceanic basalt (DRUMMOND *et al.*, 1996) or of island arc lower crustal basalt (ATHETON and PETFORD, 1993) to form felsic magma, or crystallization differentiation of basalt magma to produce felsic magma (STERN and HANSON, 1991), or partial melting of sediments to yield felsic magma (OSANAI *et al.*, 1997). The third process means that there is no genetic relationship between basic and felsic rocks. The data presented here are, however, insufficient to discuss which process is most plausible: further study, especially isotopic and radiometric studies, is needed.

The bulk rock chemistries of the phlogopite-bearing meta-ultramafic rocks are similar to the komatiitic compositions from the 2.7 Ga Munro type (Fig. 7), and their compositional variations may represent magmatic differentiation, which is probably explained by addition or subtraction of only olivine (*e.g.*, HERZBERG, 1992). A preliminary study of Nd-Sm radiometric age determination indicates the whole-rock isochron age of the phlogopite-bearing type to be about 2.7 Ga (SUZUKI, in prep.). Although the original mineral texture of the phlogopite-bearing meta-ultramafic rocks has been modified by metamorphism, their field occurrence such as forming layers and chemical features described above suggest their precursor to be a magmatic lithology with komatiitic compositions. If this is so, then the MgO-rich and SiO_2-poor samples (Figs. 7 and 8) with very low REE concentrations (Fig. 9) that correspond to the phlogopite-bearing dunite and harzburgite (Fig. 6) may represent cumulate-like rocks formed by olivine subtraction from komatiitic melts. On the other hand, the phlogopite-free meta-ultramafic rocks have bulk rock chemistries similar to peridotitic rocks such as dunite or harzburgite rather than komatiitic rocks (Figs. 7 and 8), and it is possible that their precursor may have been a depleted or residual mantle peridotite such as formed by partial melting and extraction of 40–60% peridotitic komatiitic magma (TAKAHASHI, 1990). This is consistent with the lower REE concentrations in the phlogopite-free type than in the phlogopite-bearing type, except for the cumulate-like rocks described above (Fig. 9), and with the similarity of the Nd-Sm whole-rock isochron ages (about 2.7 Ga) of the phlogopite-free type to those of the phlogopite-bearing type (SUZUKI, in prep.).

With respect to the genetic relation between the mafic gneiss and meta-ultramafic rocks, the LREE-enriched and HREE flat patterns are distinctive both in the quartz-bearing mafic gneiss and phlogopite-bearing meta-ultramafic rocks (Fig. 9), although the REE concentrations are higher in the former than in the latter. As mentioned previously, this similarity of the LREE pattern may be inherited from primary melts, namely, these rocks may be co-genetic in origin, probably the basaltic precursor of the quartz-bearing mafic gneiss representing a differentiated magma from a komatiitic magma (now represented by the phlogopite-bearing meta-ultramafic rocks), although there are compositional gaps of major and minor elements between these rocks (Figs. 7 and 8).

5. Conclusions

The ultrahigh-temperature metamorphic rocks from the Mt. Riiser-Larsen area may have been derived at least from two types of lithology, one sedimentary and the other igneous in origin. The former is now represented by the garnet felsic gneiss II and

garnet-sillimanite gneiss, and the latter by the orthopyroxene felsic gneiss, garnet felsic gneiss I, quartz-free and -bearing mafic gneisses, and phlogopite-free and -bearing meta-ultramafic rocks. Of these, the original rocks of igneous origin have various affinities such as Archaean TTG, granitic, tholeiitic, komatiitic and depleted mantle peridotitic rocks. The site of development of this variation of original rocks such as the Archaean greenstone-granite belt (*e.g.*, CONDIE, 1994) or the convergence boundary of oceanic and continental plates in the modern sense (*e.g.*, KARIG and SHARMAN, 1975) may be important for understanding the evolution of the Napier Complex as well as the Archaean craton, which will be discussed elsewhere in the near future.

Acknowledgments

We would like to express our sincere thanks to Prof. K. SHIRAISHI and Dr. Y. MOTOYOSHI for their constant encouragement and constructive discussions. We are also grateful to Drs. Y. OSANAI, M. OWADA and T. TSUNOGAE for their stimulating discussions. The journal reviewers are thanked for their critical reading of the manuscript and constructive comments.

References

ATHERTON, M.P. and PETFORD, N. (1993): Generation of sodium-rich magmas from newly underplated basaltic crust. Nature, **362**, 144–146.

BARKER, F. (1979): Trondhjemite: Definition, environment and hypotheses of origin. Trondhjemites, Dacites and Related Rocks, ed. by F. BARKER. Amsterdam, Elsevier, 1–12.

BLACK, L.P., WILLIAMS, I.S. and COMPSTON, W. (1986): Four zircon ages from one rock: the history of a 3930 Ma-old granulite from Mount Sones, Enderby Land, Antarctica. Contrib. Mineral. Petrol., **94**, 427–437.

CHANG, L.L.Y., HOWIE, R.A. and J. ZUSSMAN. (1998): Rock-Forming Minerals, Vol. 5B: Non-Silicates. 2nd ed. London, The Geological Society, 383 p.

CONDIE, K.C. (1981): Archaean Greenstone Belts. Amsterdam, Elsevier, 434 p.

CONDIE, K.C. (1985): Secular variation in the composition of basalts: An index to mantle evolution. J. Petrol., **26**, 545–563.

CONDIE, K.C. (1994): Archean Crustal Evolution. Amsterdam, Elsevier, 528 p. (Developments in Precambrian Geology, No. 11).

DALLWITZ, W.B. (1968): Coexisting sapphirine and quartz in granulite from Enderby Land, Antarctica. Nature, **219**, 476–477.

DRUMMOND, M.S., DEFANT, M.J. and KEPEZHINSKAS, P. (1996): Petrogenesis of slab-derived trondhjemite-tonalite-dasite-adakite magmas. Trans. R. Soc. Edinburgh: Earth Sci., **87**, 205–215.

ELLIS, D.J. (1980): Osumilite-sapphirine-quartz granulites from Enderby Land, Antarctica: *P-T* conditions of metamorphism, implications for garnet-cordierite equilibria and the evolution of the deep crust. Contrib. Mineral. Petrol., **74**, 201–210.

GREW, E.S. (1980): Sapphirine-quartz association from Archean rocks in Enderby Land, Antarctica. Am. Mineral., **65**, 821–836.

GREW, E.S. (1982): Osumilite in the sapphirine-quartz terrane of Enderby Land, Antarctica: Implications for osumilite petrogenesis in the granulite facies. Am. Mineral., **67**, 762–787.

HARLEY, S.L. (1987): A pyroxene-bearing meta-ironstone and other pyroxene-granulites from Tonagh Island, Enderby Land, Antarctica: further evidence for very high temperature (>980°C) Archaean regional metamorphism in the Napier Complex. J. Metamorph. Geol., **5**, 341–356.

HARLEY, S.L. and BLACK, L.P. (1997): A revised Archaean chronology for the Napier Complex, Enderby Land, from SHRIMP ion-microprobe studies. Antarct. Sci., **9**, 74–91.

HARLEY, S.L. and HENSEN, B.J. (1990): Archaean and Proterozoic high-grade terranes of East Antarctica (40–80°E): A case study of diversity in granulite facies metamorphism. High-Temperature Metamorphism and Crustal Anatexis, ed. by J.R. ASHWORTH and M. BROWN. London, Unwin Hyman, 320–370.

HERZBERG, C. (1992): Depth and degree of melting of komatiites. J. Geophys. Res., **97**, 4521–4540.

IRVINE, T.N. and BARAGAR, W.R.A. (1971): A guide to the chemical classification of the common volcanic rocks. Can. J. Earth Sci., **8**, 523–548.

ISHIZUKA, H., ISHIKAWA, M., HOKADA, T. and SUZUKI, S. (1998): Geology of the Mt. Riiser-Larsen area of the Napier Complex, Enderby Land, East Antarctica. Polar Geosci., **11**, 154–171.

KARIG, D.E. and SHARMAN, G.F. (1975): Subduction and accretion in trenches. Bull. Geol. Soc. Am., **86**, 377–389.

LAHAYE, Y. and ARNDT, N. (1996): Alteration of a komatiite flow from Alexo Ontario, Canada. J. Petrol., **37**, 1261–1284.

LUAIS, B. and HAWKESWORTH, C. (1994): The generation of continental crust: An integrated study of crust-forming processes in the Archaean of Zimbabwe. J. Petrol., **35**, 43–93.

MAKIMOTO, H., ASAMI, M. and GREW, E.S. (1989): Some geological observations on the Archean Napier Complex at Mt. Riiser-Larsen, Amundsen Bay, Enderby Land. Proc. NIPR Symp. Antarct. Geosci., **3**, 128–141.

MARTIN, H. (1987): Petrogenesis of Archaean trondhjemites, tonalites and granodiorites from eastern Finland: Major and trace element geochemistry. J. Petrol., **28**, 921–953.

MIYASHIRO, A. (1974): Volcanic rock series in island arcs and active continental margins. Am. J. Sci., **274**, 321–355.

MIYASHIRO, A. (1978): Nature of alkalic volcanic rock series. Contrib. Mineral. Petrol., **66**, 91–104.

MIYASHIRO, A. (1994): Metamorphic Petrology. University College London, UCL Press, 404p.

MOTOYOSHI, Y. and HENSEN, B.J. (1989): Sapphirine-quartz-orthopyroxene symplectites after cordierite in the Archaean Napier Complex, Antarctica: Evidence for a counterclockwise *P-T* path? Eur. J. Mineral., **1**, 467–471.

MOTOYOSHI, Y. and MATSUEDA, H. (1984): Archean granulites from Mt. Riiser-Larsen in Enderby Land, East Antarctica. Mem. Natl Inst. Polar Res., Spec. Issue, **33**, 103–125.

MOTOYOSHI, Y. and MATSUEDA, H. (1987): Corundum+quartz association in Archean granulite-facies rock from Enderby Land, East Antarctica: Preliminary interpretation. Proc. NIPR Symp. Antarct. Geosci., **1**, 107–112.

MOTOYOSHI, Y. and SHIRAISHI, K. (1995): Quantitative chemical analyses of rocks with X-ray fluorescence analyzer: (1) Major elements. Nankyoku Shiryô (Antarct. Rec.), **39**, 40–48.

MOTOYOSHI, Y., HENSEN, B. J. and MATSUEDA, H. (1990): Metastable growth of corundum adjacent to quartz in a spinel-bearing quartzite from the Archaean Napier Complex, Antarctica. J. Metamorph. Geol., **8**, 125–130.

MOTOYOSHI, Y., ISHIZUKA, H. and SHIRAISHI, K. (1996): Quantitative chemical analyses of rocks with X-ray fluorescence analyzer: (2) Trace elements. Nankyoku Shiryô (Antarct. Rec.), **40**, 53–63.

OSANAI, Y., OWADA, M., SHIMURA, T., KAWASAKI, T. and HENSEN, B.J. (1997): Crustal anatexis and related acidic magma genesis in the Hidaka metamorphic belt, Hokkaido, northern Japan. Mem. Geol. Soc. Jpn., **47**, 29–42 (in Japanese with English abstract).

ROLLINSON, H. (1999): Petrology and geochemistry of metamorphosed komatiites and basalts from the Sula Mountains greenstone belt, Sierra Leone. Contrib. Mineral. Petrol., **134**, 86–101.

SANDIFORD, M. and POWELL, R. (1986): Pyroxene exsolution in granulites from Fyfe Hills, Enderby Land, Antarctica: Evidence for 1000°C metamorphic temperatures in Archean continental crust. Am. Mineral., **71**, 946–954.

SHERATON, J.W. (1984): Chemical changes associated with high-grade metamorphism of mafic rocks in the East Antarctic Shield. Chem. Geol., **47**, 135–157.

SHERATON, J.W., TINGEY, R.J., BLACK, L.P., OFFE, L.A. and ELLIS, D.J. (1987): Geology of Enderby Land and Western Kemp Land, Antarctica. BMR Bull., **223**, 51 p.

SHAW, D.M. (1972): The origin of the Apsley gneiss, Ontario. Can. J. Earth Sci., **9**, 18–35.

STERN, R.A. and HANSON, G.N. (1991): Archean high-Mg granodiorite: A derivative of light rare earth element-

enriched monzodiorite of mantle origin. J. Petrol., **32**, 201–238.

SUN, S.-S. and NESBITT, R.W. (1978): Petrogenesis of Archaean ultrabasic and basic volcanics: Evidence from rare earth elements. Contrib. Mineral. Petrol., **65**, 301–325.

SUN, S.-S. and MCDONOUGH, W.F. (1989): Chemical and isotopic systematics of oceanic basalts: Implications for mantle composition and processes. Magmatism in the Ocean Basins, ed. by A.D. SAUNDERS and M.J. NORRY. Oxford, Blackwell, 313–345 (Geol. Soc. Spec. Publ., No. 42).

TAKAHASHI, E. (1990): Speculations on the Archean mantle: Missing link between komatiite and depleted garnet peridotite. J. Geophys. Res., **95**, 15941–15954.

TARNEY, J. and WINDLEY, B.F. (1977): Chemistry, thermal gradients and evolution of the lower continental crust. J. Geol. Soc. London, **134**, 153–172.

(Received April 3, 1999; Revised manuscript accepted May 24, 1999)